

1 **Title:** Vasculature-on-a-chip Technologies as Platforms for Advanced Studies of Bacterial
2 Infections

3

4 **Authors:** Lily Isabelle Gaudreau¹, Elizabeth J. Stewart^{1,2*}

5 1. Chemical Engineering, Worcester Polytechnic Institute, Worcester, MA

6 2. Biomedical Engineering, Worcester Polytechnic Institute, Worcester, MA

7 *Corresponding Author, ejstewart@wpi.edu

8 **Abstract**

9 Bacterial infections frequently occur within or near the vascular network as the vascular network
10 connects organ systems and is essential in delivering and removing blood, essential nutrients,
11 and waste products to and from organs. In turn, the vasculature plays a key role in the host
12 immune response to bacterial infections. Technological advancements in microfluidic device
13 design and development have yielded increasingly sophisticated and physiologically relevant
14 models of the vasculature including vasculature-on-a-chip and organ-on-a-chip models. This
15 review aims to highlight advancements in microfluidic device development that have enabled
16 studies of the vascular response to bacteria and bacterial-derived molecules at or near the
17 vascular interface. In the first section of this review, we discuss the use of parallel plate flow
18 chambers and flow cells in studies of bacterial adhesion to the vasculature. We then highlight
19 microfluidic models of the vasculature that have been utilized to study bacteria and bacterial-
20 derived molecules at or near the vascular interface. Next, we review organ-on-a-chip models
21 inclusive of the vasculature and pathogenic bacteria or bacterial-derived molecules that stimulate
22 an inflammatory response within the model system. Finally, we provide recommendations for
23 future research in advancing the understanding of host-bacteria interactions and responses during
24 infections as well as in developing innovative antimicrobials for preventing and treating bacterial
25 infections that capitalize on technological advancements in microfluidic device design and
26 development.

27 **1. Introduction**

28 The vascular network is essential for the transportation of blood and delivery of oxygen
29 and nutrients to tissues as well as in the removal of cellular and metabolic waste products
30 throughout the body¹. Additionally, the vascular network serves as a connecting network
31 between organs. The vasculature and the blood cells contained within the vascular network are
32 essential components of the host immune response to bacterial infections.

33 During infections, pathogenic bacteria interface with the vasculature in direct and indirect
34 ways. Bacteria come into direct contact with the vasculature during catheter-associated
35 infections, bloodstream infections, secondary infections, infections of deep wounds and surgical
36 incisions, infective endocarditis, and bacterial meningitis (Fig. 1). The adhesion of bacteria to
37 the vasculature is mediated by surface proteins of both bacteria and the vascular endothelium² as
38 well as fluid flow within the vascular network³. Bacteria located within tissues can also cue an
39 inflammatory response of the vascular endothelium that signals the recruitment of immune cells
40 to an infection site⁴. Additionally, bacterial-derived molecules within the bloodstream or within
41 host tissues can activate an inflammatory response from the vascular endothelium². Bacterial-
42 derived molecules or components with structural motifs recognized by host cell receptors are
43 known as pathogen-associated molecule patterns (PAMPs)⁵.

44 The first studies of bacterial-vascular interactions used parallel plate flow chambers or
45 microfluidic flow cells inclusive of vascular endothelial cell monolayers to reveal mechanisms of
46 bacterial adhesion to the vasculature. Technological advancement in microfluidic device design
47 and fabrication has enabled the development of more sophisticated *in vitro* models of the
48 vasculature and in turn advanced studies of bacterial infections at or near the vascular interface.
49 Recent developments in vascularized bacterial infection models include three-dimensional

50 vasculature-on-a-chip microphysiological systems and organ-on-a-chip models with vascular
51 monolayers interfacing with relevant host tissues that incorporate bacteria or bacterial-derived
52 molecules. The incorporation of bacteria or bacterial-derived molecules into technologically
53 advanced vascularized microfluidic models creates opportunities for gaining new mechanistic
54 insight into how bacteria interact with the vasculature during infection and in developing novel
55 antimicrobial therapeutics to prevent and treat bacterial infections.

56 The overall goal of this review article is to provide perspective on how technological
57 advancements in microfluidics have enabled new insights into the role of the vasculature in the
58 host response to bacterial infections and highlight how continued innovation in microfluidic
59 technologies will pave the way for new directions of research in the pathogenesis of bacterial
60 infections and the development of bacterial infection prevention and control strategies. This
61 review starts by introducing research insights gained by studying bacterial adhesion to the
62 vascular endothelium in parallel plate flow chambers and microfluidic flow cells (Section 2).
63 Next, we review microfluidic models of the vasculature utilized to study the response of the
64 vascular endothelium and immune cells to bacterial infections at or near the vascular interface
65 (Section 3). We then highlight organ-on-a-chip technologies inclusive of the vasculature that
66 have modeled bacterial infections (Section 4). Finally, we discuss future opportunities for
67 utilizing vascularized microfluidic models to advance the scientific understanding of the
68 pathogenesis of bacterial infections and inform the development of innovative infection
69 prevention and control technologies (Section 5).

70

71 **2. Parallel plate flow chambers and flow cells for studying bacteria-vascular interactions**

72 Parallel plate flow chambers for studying the vascular response to fluid flow were first
73 developed in the 1970s⁶. Parallel plate flow chambers generally consist of a lower plate
74 containing a glass slide for cell culture and an upper polycarbonate plate with inlet and outlet
75 ports for media flow. The two plates are separated by a silicon gasket of ~200-250 μm . Parallel
76 plate flow chambers and commercial flow cells with similar geometries have been the primary
77 models for advancing the understanding of bacterial adhesion to the vasculature under flow as
78 these models enable study of bacterial adhesion to vascular monolayers at physiological shear
79 stress. As vascular cells are sensitive to shear stress their properties are maintained when grown
80 at physiological shear stress, including cellular morphology, alignment, barrier properties, and
81 signaling pathways^{7,8,9}. The inclusion of a vascular endothelium with physiologically relevant
82 properties is important in studies of bacterial-vascular interactions.

83 Bacterial adhesion to the vasculature while undergoing shear stress has been studied
84 using both parallel plate flow chambers and flow cells. Parallel plate flow chambers have
85 revealed that *Staphylococcus aureus* adhesion to the vascular endothelium significantly
86 decreases at physiological shear stress on a non-activated vascular endothelial monolayer^{10, 11}.
87 However, when the endothelial monolayer is activated, von Willebrand factor expression on the
88 endothelial surface mediates the binding of *S. aureus*^{12, 13, 14} and *Streptococcus pneumoniae*¹⁵ to
89 the vascular endothelium at physiological shear stress. Parallel plate flow chambers have also
90 been used to demonstrate that adhesion of *Neisseria meningitidis* to the vascular endothelium
91 occurs at the low shear stresses found in capillaries but not in the higher shear stresses typical of
92 the bloodstream, which aligns with clinical observations of the localization of meningococcus
93 attachment to capillaries during meningitis¹⁶. Collectively, these studies demonstrate how
94 parallel plate flow chambers and flow cells have been used to show how shear stress, vascular

95 response, and bacterial proteins contribute to preventing or promoting bacterial adhesion to the
96 vasculature.

97 In addition to direct interactions with bacteria, the vascular endothelium is responsive to
98 bacterial-derived molecules, such as the PAMP lipopolysaccharide (LPS). The response of the
99 vascular endothelium to LPS and shear stress has been studied using parallel plate flow
100 chambers. Zeng et al. found that at high physiological shear stress the vascular endothelium
101 can resist LPS-induced apoptosis as compared to static cultures using the same concentration of
102 LPS to stimulate the vascular endothelium ¹⁷. Additionally, they found that shear stress reduced
103 the expression of the pro-inflammatory cytokine interleukin 6 (IL-6) by the vascular endothelium
104 during LPS stimulation ¹⁷. In another study, Ploppa et al. revealed that stimulation of both the
105 vascular endothelium and neutrophils by LPS resulted in reduced neutrophil adhesion to the
106 vascular endothelium at high shear stress ¹⁸. These studies show that parallel plate flow
107 chambers are useful for identifying how shear stress modulates the response of the vascular
108 endothelium to LPS stimulation.

109 Parallel plate flow chambers are a beneficial tool for studying bacterial-vasculature
110 interactions as they enable the development of well-defined uniform shear stresses, direct
111 visualization of bacteria and the vasculature, and straightforward sampling of secreted factors ¹⁹.
112 One limitation of parallel plate flow chambers is the two-dimensional geometry of the vascular
113 endothelial monolayer. Another limitation specific to using parallel plate flow chambers for
114 studying bacteria is that they require large volumes of media to maintain high shear stress during
115 experiments, as media cannot be recirculated in parallel plate flow chambers containing bacteria.
116 In experiments with only vascular cells, media can be recirculated within the flow chambers to
117 mitigate the use of high media volumes while maintaining high shear stress. Recirculation of

118 media in a system containing bacteria for studies longer than the doubling time of the bacteria is
119 problematic as bacteria will be continually introduced to the system from the media reservoir.
120 Thus, parallel plate flow chambers are valuable for studies of bacterial adhesion but not suitable
121 for studies of the progression of bacterial infections.

122

123 **3. Vasculature-on-a-chip devices for studying Bacterial-Vascular Interactions**

124 This section highlights microfluidic models that incorporate either intact bacteria or
125 bacterial-derived molecules at or near the vascular interface for investigating how bacterial
126 interactions with the vascular endothelium prompt inflammation and immune cell recruitment.

127

128 **3.1 Microfluidic models containing bacteria and the vasculature**

129 There are a limited number of microfluidic models that have been developed to study the
130 interactions between intact bacteria and the vasculature. During an infection, bacterial cells can
131 be found within bloodstream, at the vascular interface or at an infection site, such as a specific
132 tissue or medical device. Microfluidic models including intact bacteria have recapitulated
133 bacterial transmigration from the bloodstream across the vasculature as well as immune cell
134 recruitment from the bloodstream to an infection site (Fig. 2A-B, Table 1).

135 Utilizing transwell dishes as design inspiration, Bergevin et al. developed a
136 transmembrane microfluidic device that enabled the direct visualization of bacterial
137 extravasation²⁰. The device was designed such that endothelial cells could be grown at
138 physiological shear stresses on the bottom surface of a polyethylene terephthalate (PET)
139 membrane that was located between a lower channel and an upper observation chamber²⁰.
140 Bacteria were added to the device via the lower channel containing endothelial cells and direct

PLEASE CITE THIS ARTICLE AS DOI: 10.1063/5.0179281

141 visualization of bacteria transmigration across the endothelial monolayer was observed²⁰. This
142 study enabled advances in understanding bacterial transendothelial migration out of the
143 bloodstream and into the surrounding tissue²⁰.

144 Intact bacteria have also served as a cue for stimulating the migration of neutrophils
145 across the endothelial lumen. Hind et al. developed a model of neutrophil migration across a
146 three-dimensional, endothelial cell lined lumen²¹. The vessel was embedded within an
147 extracellular matrix (ECM) and neutrophils migrated toward an intact *Pseudomonas aeruginosa*
148 bacterial source located exterior to the extracellular matrix²¹. This model revealed that
149 neutrophils can migrate towards bacteria for up to 24 hours and that endothelial cell secretion of
150 IL-6, a pro-inflammatory cytokine, was important for mediating neutrophil migration as blocking
151 IL-6 decreased neutrophil migration²¹. The endothelial lumen was required to see neutrophil
152 response, as there was negligible migration when the vessel was not vascularized²¹.
153 Additionally, using intact bacteria in the model increased the overall number of migrating
154 neutrophils and the distance of neutrophil migration compared to the use of the chemoattractants
155 N-Formyl-methionyl-leucyl-phenylalanine (fMLP) and interleukin 8 (IL-8)²¹. This model
156 enabled scientific advancement of the understanding of how the vascular endothelium
157 contributes to neutrophil migration and survival during bacterial infections²¹.
158

159 **3.2 Microfluidic models containing bacterial-derived molecules and the vasculature**

160 Bacterial-derived molecules have been incorporated into microfluidic devices containing
161 vascular monolayers to stimulate the inflammatory response of the endothelium or as a
162 chemoattractant for recruiting immune cells across the vascular endothelium (Fig. 2C-G, Table
163 2). The first scenario represents the release of bacterial products into the bloodstream, whereas

164 the second scenario represents the recruitment of immune cells to an infection site. LPS, an
165 inflammatory PAMP derived from the outer membrane of Gram-negative bacteria ²², and fMLP,
166 a chemoattractant for neutrophils derived from Gram-negative and Gram-positive bacteria ²³, are
167 the primary molecules used within these two types of infection models.

168

169 *Lipopolysaccharide (LPS) within microfluidic models of the vasculature*

170 LPS has been used to stimulate the inflammatory response of endothelial cells within
171 microfluidic models of the vasculature. These models have provided new insights into immune
172 cell recruitment to the vascular endothelium during inflammation and factors that protect the
173 barrier integrity of the vascular endothelium during activation by LPS.

174 Immune cell recruitment due to LPS gradients outside of the vasculature has been
175 modeled experimentally in a microfluidic device. Nam et al. developed a three-dimensional
176 microfluidic model with three channels, where channel one contained an endothelial cell
177 monolayer, channel two contained a collagen hydrogel, and channel three was a media reservoir
178 with LPS ²⁴. In this study, monocytes were introduced within the endothelial cell lumen and
179 migrated across the endothelial cell monolayer through the collagen toward the LPS ²⁴.

180 Monocyte migration distance through the ECM increased in the presence of LPS ²⁴.

181 Additionally, barrier function of the vascular endothelium was evaluated as a marker of
182 inflammatory response, where barrier integrity was disrupted when LPS was present as indicated
183 by downregulation of vascular endothelial cadherin (VE-cadherin), a cell-cell adhesion molecule
184 between endothelial cells ²⁴. Intercellular adhesion molecule 1 (ICAM-1), an adhesion molecule
185 necessary for immune cell adhesion to the vasculature prior to transmigration through the
186 vasculature to an infection site, was also upregulated when LPS was present within the system ²⁴.

PLEASE CITE THIS ARTICLE AS DOI: 10.1063/5.0179281

187 This study recapitulated the inflammatory response of blood vessels and monocyte migration
188 across blood vessels due to diffusion of LPS through the extracellular matrix on the exterior of a
189 blood vessel ²⁴.

190 Microfluidic models have also been utilized to evaluate endogenous mechanisms and
191 pharmaceutical treatments for preserving endothelial cell barrier integrity in response to
192 inflammation by LPS. The glycocalyx is the outermost surface layer of the endothelium ²⁵.

193 Glycocalyx shedding contributes to the breakdown of the integrity of the endothelium barrier and
194 can occur during bloodstream infections. Kiyan et al. established a microfluidic model for
195 evaluating the protective nature of heparanase-2, an endogenous inhibitor of an enzyme that
196 targets heparan sulfate, in preserving the integrity of the endothelial glycocalyx during activation
197 of endothelial cells by LPS ²⁶. In a simple flow cell model inclusive of an endothelial monolayer
198 on a coverglass, heparinase-2 was shown to help maintain the endothelial cell barrier, as
199 evidenced by preservation of VE-cadherin cell-cell contacts when heparinase-2 is over-expressed
200 by endothelial cells, reduction of pro-inflammatory cytokine expression by endothelial cells and
201 reduction of toll-like receptor 4 (TLR-4) activation by LPS ²⁶. This study revealed a protective
202 role of an endogenous enzyme, heparinase-2, in microvascular inflammation. In another flow
203 cell model, Liao et al. demonstrated that the medication dexmedetomidine (DEX) was able to
204 ameliorate the degradation of the glycocalyx and inhibit the loss of VE-cadherin expression
205 typically observed during LPS treatment ²⁷. This study revealed that DEX can serve as a
206 protective agent for the glycocalyx and endothelium during LPS exposure ²⁷.

207

208 *N*-Formyl-methionyl-leucyl-phenylalanine (*f*MLP) within microfluidic models of the vasculature

209 fMLP has been used as a neutrophil chemoattractant within microfluidic models to study
210 neutrophil chemotaxis in the presence of endothelial cells and transendothelial migration of
211 neutrophils through an endothelial cell monolayer. These models shed new light on neutrophil-
212 endothelial interactions during neutrophil recruitment to an infection site.

213 In the simplest microfluidic models of neutrophil chemotaxis, a chemoattractant gradient
214 is created in a solution adjacent to an endothelial monolayer. In one such model, Kim et al. used
215 serpentine channels to create a fMLP concentration gradient within media flowing across an
216 observation channel containing endothelial cells and revealed that neutrophil chemotaxis occurs
217 towards the fMLP with and without a competing chemoattractant gradient²⁸. In another
218 microfluidic model, Soroush et al. utilized digitized microvascular networks to create channel
219 geometries based on the microvasculature within mouse cremaster muscles²⁹. The networked
220 channels were then divided into three parallel compartments with the first compartment
221 containing vascular cells, the second compartment consisting of a porous barrier, and the third
222 compartment acting as a mock “tissue compartment” filled with media containing a
223 chemoattractant²⁹. This microfluidic model was used to demonstrate that protein kinase C δ
224 plays a key role in regulating neutrophil migration by decreasing the adhesion and migration of
225 neutrophils across endothelial cells in response to fMLP²⁹.

226 Three-dimensional models of neutrophil chemotaxis generally include a vascular
227 monolayer adjacent to an extracellular matrix containing a concentration gradient of
228 chemoattractant. The specific geometry of the devices and the orientation of the chemoattractant
229 gradients vary by model. In one three-dimensional model, Han et al. found that a vascular
230 endothelial monolayer was required for significant neutrophil migration into a collagen hydrogel
231 indicating that endothelial-neutrophil interactions are critical for neutrophil migration to an

232 infection site ³⁰. In a different three-dimensional model of neutrophil chemotaxis, Wu et al.
233 learned that neutrophil migration across endothelial cells into a collagen hydrogel is dependent
234 on the spatial gradient and concentration of the chemoattractant within the extracellular matrix
235 material, and demonstrated synergistic effects between different chemoattractants ³¹. In another
236 three-dimensional model inclusive of microchannels with bifurcations and curvatures, Menon et
237 al. found that chemoattractant gradients across a collagen hydrogel significantly increased
238 neutrophil migration ³². Neutrophils consistently are recruited across the endothelial-
239 extracellular matrix interface when a chemoattractant gradient is present in the extracellular
240 matrix.

241 Three-dimensional models of neutrophil chemotaxis toward fMLP have also been
242 employed to reveal how primary vascular cells and extracellular matrix influence neutrophil
243 migration through the vascular endothelium. Ingram et al. utilized a microfluidic model
244 containing a three-dimensional endothelial cell lumen embedded within a collagen hydrogel with
245 fMLP added to a channel on the exterior of the hydrogel as a chemoattractant to show neutrophil
246 extravasation and migration responses ³³. A unique feature of this model was the use of induced
247 pluripotent stem cells (iPSC)-derived cells as a more physiologically relevant source of
248 endothelial cells ³³. Additionally, differences between purified neutrophil migration and
249 neutrophil migration from whole blood were assessed in this model, where purified neutrophil
250 migration distances were reduced compared to the migration distances of neutrophils from whole
251 blood when fMLP was used as the model chemoattractant ³³. In another study, Riddle et al. used
252 a three-dimensional model with an endothelial vessel in contact with extracellular matrix to
253 investigate differences in neutrophil transmigration toward fMLP through endothelial cells
254 surrounded by either collagen or geltrex matrices ³⁴. This study determined that fMLP was

255 required for neutrophil transmigration into collagen, whereas transmigration occurred without
256 fMLP in the geltrex matrix indicating that extracellular components play a key role in
257 influencing cellular behaviors ³⁴.

258

259 **4. Organ-on-a-chip infection models inclusive of vasculature**

260 Organ-on-a-chip models have emerged as a novel method for recapitulating organ
261 behaviors *in vitro* and are beginning to be used to study host-pathogen interactions during the
262 progression of infectious disease. The initial use of organ-on-a-chip models to study interactions
263 between pathogenic bacteria and the gut, lung, bladder, and placenta has been reviewed
264 elsewhere ^{35, 36, 37, 38}. As the vascular system interfaces with organs throughout the body, many
265 organ-on-a-chip models include an interface within the microfluidic device between the specific
266 organ tissue being modeled and the vascular endothelium. This section of our review focuses on
267 providing an overview of organ-on-a-chip models inclusive of vasculature that study the
268 responses of organ systems to intact bacteria or bacterial-derived molecules. Organ-on-a-chip
269 models inclusive of the vasculature and pathogenic bacteria or bacterial-derived molecules have
270 been developed for the lung, gut, brain, lymphatic system, liver, bladder, and placenta (Fig. 3).
271 Scientific findings utilizing these microfluidic models range from the effects of bacterial
272 infections or bacterial-induced inflammation on organ tissues to specific biological mechanisms
273 tied to cellular responses to infection.

274

275 **4.1 Organ-on-a-chip infection models inclusive of vasculature and bacteria**

276 Organ-on-a-chip models inclusive of the vasculature have been used to investigate the
277 effect of intact bacteria on immune cell recruitment and cellular responses during both

278 bloodstream and organ specific infections (Fig. 4, Table 3). These studies frequently include
279 reports on the effects of bacteria on the barrier function of the vascular endothelium and cellular
280 expression of inflammatory markers. This section highlights studies of neutrophil transmigration
281 and macrophage responses to intact bacteria using various organ-on-a-chip models.
282 Additionally, this section reviews an organ-on-a-chip model with added functionality for
283 monitoring cellular response to bacterial infection and a disease-on-a-chip model for examining
284 interactions between bacteria and diseased organs.

285 Neutrophil transmigration from the vascular endothelium to an infection site has been
286 studied using organ-on-a-chip models of the lung, lymphatic system, and bladder. Huh et al.
287 developed a lung-on-a-chip representative of the alveolar-capillary interface with alveolar
288 epithelial cells and vascular endothelial cells grown on opposite sides of a thin, porous
289 membrane and studied transmigration of neutrophils from the endothelial microchannel into the
290 alveolar channel during an *Escherichia coli* infection of the alveolar channel³⁹. After five hours
291 of infection, the vascular endothelium was activated as evidenced by the transmigration of
292 neutrophils across the capillary-alveolar interface³⁹. After transmigration, the neutrophils
293 migrated toward the *E. coli* and engulfed the bacteria until most bacteria were cleared from the
294 channel, recapitulating an integrated cellular immune response to lung infections³⁹. In another
295 study of neutrophil extravasation during bacterial infection using an organ-on-a-chip model,
296 McMinn et al. created a microfluidic model of the lymphatic system that included parallel
297 lumens of lymphatic endothelial cells and vascular endothelial cells embedded in a hydrogel,
298 where *Pseudomonas aeruginosa* was added to the lymphatic endothelial lumen and neutrophils
299 were added to the vascular endothelial lumen⁴⁰. In this lymphatic system model, neutrophil
300 extravasation occurred across the vascular endothelium and neutrophils subsequently migrated

301 toward *P. aeruginosa*⁴⁰. There were variations in the occurrence of transendothelial migration
302 based on the cells present in the model, indicating that modulation of cellular secretion factors
303 transpires due to crosstalk between the lymphatic and vascular endothelium⁴⁰. Sharma et al.
304 studied the dynamics of neutrophil recruitment to the site of infection from the bloodstream
305 using a bladder-on-a-chip model representative of a urinary tract infection⁴¹. The model was
306 comprised of the epithelial-vascular interface where bladder epithelial cells and vascular
307 endothelial cells were cultured on opposite sides of a porous membrane with *E. coli* added to the
308 channel with bladder cells and neutrophils added to the channel with endothelial cells⁴¹. The
309 neutrophils in the bladder-on-a-chip model migrated across the endothelium to the bacteria
310 source and subsequently formed neutrophil extracellular traps⁴¹. There was also an increase in
311 ICAM-1 expression by the endothelial cells and an increase in the release of inflammatory
312 cytokines from the bladder and endothelial cells in response to the bacteria in the bladder-on-a-
313 chip model⁴¹.

314 Evaluation of macrophage response and recruitment to bacterial infections has been
315 performed using organ-on-a-chip models of the liver, lung, and placenta. Siwczak et al.
316 developed a liver-on-a-chip with endothelial cells and hepatocytes grown on opposite sides of a
317 porous membrane and macrophage at the interface between the endothelial cell layer and the
318 parenchymal cell layer formed by the hepatocytes⁴². *Staphylococcus aureus* was introduced to
319 the vascular channel on the liver-on-a-chip to represent a bloodstream infection⁴². *S. aureus*
320 cells were sequestered to the macrophage and cleared from circulation within the model⁴². As a
321 result, the macrophage response protected the endothelial cells and hepatocytes from becoming
322 infected with bacteria⁴². M2 polarization of macrophage, prior to infection, resulted in the
323 highest bacterial cell counts within macrophage with a preference for small colony variants of *S.*

324 *aureus*⁴². This study revealed a specific role of M2 macrophage as a niche for facilitating *S.*
325 *aureus* persistence during bacterial infection of the liver⁴². Deinhardt-Emmer et al. created an
326 alveolus-on-a-chip model inclusive of macrophage at the alveolar-endothelial interface to study
327 co-infections of *S. aureus* and influenza virus⁴³. Infection of the alveolar channel induces an
328 inflammatory response of the endothelium in both bacterial infections and bacterial and influenza
329 co-infections⁴³. Additionally, bacteria are found to translocate from the alveolar channel to the
330 endothelial channel during co-infections⁴³. In another organ-on-a-chip infection model
331 containing macrophage, Zhu et al. established a placenta-on-a-chip to study the response of the
332 placenta to an *E. coli* infection originating on the maternal side of the placenta⁴⁴. The placenta-
333 on-a-chip consisted of trophoblasts and vascular endothelial cells grown on opposite sides of a
334 thin, porous membrane to represent the maternal and fetal side of the placental barrier,
335 respectively, with *E. coli* added to the trophoblast channel⁴⁴. The addition of *E. coli* to the
336 model resulted in significant cell death of both the trophoblasts and endothelial cells⁴⁴. This also
337 corresponded with an increase in inflammatory cytokine expression and barrier disruption of the
338 fetal endothelial cells when the trophoblasts were present in the model, indicating cell-to-cell
339 communication between the maternal and fetal cells⁴⁴. In addition, macrophage added to the
340 maternal channel after *E. coli* infection migrated and attached to the trophoblast surface, which
341 increased inflammatory cytokine expression in response to infection⁴⁴.

342 Cellular responses can be monitored in real-time on microfluidic devices by integrating
343 biosensors into the chip. One example of an infection model with an integrated biosensor is a
344 neurovascular-unit-on-a-chip, where a microelectrode array (MEA) was integrated into the chip
345 design to enable monitoring of the neuronal response to a bacterial infection representative of
346 bacterial meningitis⁴⁵. The neurovascular-unit-on-a-chip consisted of two chambers separated

347 by a porous membrane with vascular endothelial cells cultured directly on the porous membrane
348 in the upper chamber and cortical neurons cultured on the MEA situated at the lower wall of the
349 lower chamber ⁴⁵. After *E. coli* was added to the vascular chamber, the barrier permeability of
350 the endothelial layer was reduced within four hours, while the neuronal electrical activity
351 decreased 20 hours after infection ⁴⁵. The duration of time for the decrease in neuronal electrical
352 activity was five times longer when the endothelial vasculature was included with the cortical
353 neurons in the model indicating a protective role of the vasculature during bacterial meningitis ⁴⁵.

354 Bacterial infections of healthy and diseased lungs were recapitulated using lung-on-a-
355 chip models. Plebani et al. developed a model of cystic fibrosis (CF) by modifying a lung-on-a-
356 chip model to include cystic fibrosis bronchial epithelial cells ⁴⁶. Bronchial epithelial cells and
357 vascular endothelial cells were grown in two channels on opposite sides of a porous membrane
358 ⁴⁶. *P. aeruginosa* was added to the channel with bronchial epithelial cells and
359 polymorphonuclear leukocytes (PMNs) were added to the vascular endothelial channel ⁴⁶. In the
360 CF model, there were a higher number of bacteria embedded in the mucus layer of the
361 epithelium and a higher number of PMNs adhered to the endothelium than in the healthy model;
362 however, there was an increase in inflammatory cytokine expression by vascular endothelial
363 cells on both microfluidic chips ⁴⁶.

364

365 **4.2 Organ-on-a-chip infection models inclusive of vasculature and bacterial-derived
366 molecules**

367 Inflammation and inflammatory responses of organ tissues and vasculature due to
368 bacterial-derived molecules have been studied using organ-on-a-chip models (Fig. 5, Table 4).
369 Bacterial-derived molecules, such as LPS, can be added to the vascular channel or to the organ

PLEASE CITE THIS ARTICLE AS DOI: 10.1063/5.0179281

370 tissue channel of a device to mimic bacterial-derived inflammatory cues within the bloodstream
371 or to represent an infection within an organ, respectively. Organ-on-a-chip models inclusive of
372 bacterial-derived molecules have been used to investigate immune cell recruitment and response
373 during infection, mechanistic insights into the inflammatory response of the vascular
374 endothelium, pulmonary thrombosis, and differences between the responses of healthy and
375 diseased organ tissue to bacterial-derived inflammatory cues.

376 Neutrophil recruitment due to stimulation with LPS in a liver-on-a-chip shows evidence
377 of crosstalk between liver cells during neutrophil recruitment. Du et al. developed a liver-on-a-
378 chip model consisting of two channels separated by a porous membrane with liver sinusoidal
379 endothelial cells (LSECs) and Kupffer cells (KCs) co-cultured on the membrane in the upper
380 channel, hepatic stellate cells cultured on opposite side of the membrane in the lower channel,
381 and hepatocytes cultured on the far wall of the lower channel.⁴⁷. LPS and neutrophils were both
382 added to the endothelial cell channel⁴⁷. LPS stimulation of the endothelium in the liver-on-a-
383 chip increased neutrophil adhesion to the endothelial surface by 63% and increased neutrophil
384 aggregate size compared to neutrophil adhesion to a monoculture of LSECs stimulated by LPS
385⁴⁷. This indicates that cross talk between liver cells increases neutrophil recruitment to the
386 vascular endothelium⁴⁷.

387 Monocyte response to infection has also been investigated in organ-on-a-chip models.
388 Kim et al. studied interactions between LPS stimulation and peripheral blood mononuclear cells
389 (PBMCs)—a combination of monocytes, macrophages, lymphocytes, Natural Killer cells, and
390 dendritic cells⁴⁸—in a gut-on-a-chip model⁴⁹. The gut-on-a-chip model included intestinal
391 epithelial cells and vascular endothelial cells on opposite sides of a flexible, porous membrane⁴⁹.
392 LPS was added to intestinal epithelial chamber and PBMCs were added to the endothelial cell

PLEASE CITE THIS ARTICLE AS DOI: 10.1063/5.0179281

393 chamber ⁴⁹. Inclusion of LPS and PBMCs in the model was necessary for activation of
394 endothelial cells and PBMC adhesion to the endothelium, demonstrating cellular cross talk is
395 important for the initiation of an immune response in the gut-on-a-chip model ⁴⁹. In a study of
396 specific roles of monocytes in sepsis-related liver dysfunction, Gröger et al. stimulated a liver-
397 on-a-chip containing monocytes with LPS and found that monocytes attenuate inflammation-
398 related cell responses in the liver model ⁵⁰. The liver-on-a-chip model included two channels
399 separated by a porous membrane ⁵⁰. The upper channel contained vascular endothelial cells co-
400 cultured with macrophage on a suspended porous membrane and the lower channel contained a
401 hepatic cell layer comprised of hepatocytes and hepatic stellate cells cultured on the bottom
402 channel wall with a media-filled space between the porous membrane and the hepatic cells in the
403 lower channel ⁵⁰. After LPS addition to the liver-on-a-chip, monocytes are recruited to the
404 endothelium and transmigrate to the hepatic compartment, the endothelium barrier is disrupted,
405 and the endothelium increases inflammatory cytokine expression ⁵⁰. The presence of the
406 endothelial cells and macrophage in the liver-on-a-chip decreases the susceptibility of
407 hepatocytes to LPS stimulation, indicating that cellular cross talk between macrophage, the
408 vasculature, and hepatic cells contributes to the inflammatory response to LPS in the liver ⁵⁰.

409 In a more mechanistic study, a blood-brain-barrier-on-a-chip was utilized to demonstrate
410 that LPS stimulation of the vascular channel adjacent to human astrocytes reduced the barrier
411 integrity of the vasculature ⁵¹. Additionally, this study revealed that LPS stimulation of
412 vasculature increased expression of miR-146a, a microRNA expressed in the central nervous
413 system associated with an inflammatory response ⁵¹.

414 Organ-on-a-chips can be used to evaluate the response of both diseased and healthy
415 tissues to inflammation due to bacterial-derived molecules. A lung-on-a-chip model of

PLEASE CITE THIS ARTICLE AS DOI: 10.1063/5.0179281

416 pulmonary thrombosis incorporated whole blood into the model to study the development of
417 thrombosis during LPS stimulation ⁵². The lung-on-a-chip included two microchannels separated
418 by a thin membrane with primary human lung alveolar epithelial cells grown on the thin
419 membrane in the upper channel and vascular endothelial cells on all four channel walls to create
420 a three-dimensional microvessel in the lower channel ⁵². After LPS addition to the channel with
421 alveolar epithelial cells, the permeability of the tissue-tissue interface increased, platelet binding
422 to the endothelium increased, and inflammatory cytokine expression increased; however, this did
423 not occur when LPS was added to the endothelial cell channel, indicating that tissue-tissue
424 interactions between the lung alveolar epithelium and the vascular endothelium contribute to the
425 induction of pulmonary thrombosis by LPS ⁵². The response of healthy and diseased lungs to a
426 bacterial-derived molecule can be elucidated using lung-on-a-chip models. In one such example,
427 Benam et al. developed a chronic obstructive pulmonary disease (COPD) model, where COPD-
428 patient derived primary human airway epithelial cells and human lung microvascular endothelial
429 cells were cultured on opposite sides of a porous membrane to create a tissue-tissue interface
430 within a microfluidic device ⁵³. Comparisons between COPD and healthy lung-on-a-chip models
431 revealed that LPS exacerbated cells on the COPD chip as indicated by the upregulation of
432 inflammatory cytokines on the COPD chip ⁵³.

433

434 **5. Future Directions and Opportunities**

435 The measurable advancements in microfluidic models of bacterial infections at the vascular
436 interface open the door to future research directions in infection pathogenesis, device
437 development, and antimicrobial discovery. Variations in the biological elements included within

438 the devices, such as the bacterial strains, bacterial-derived molecules, or mammalian cell sources,
439 integration of technological advancements realized through the development of other
440 microphysiological systems, and application of the model to develop and evaluate novel
441 antimicrobial solutions are all future opportunities for utilizing microfluidic models of bacterial
442 infections at the vascular interface.

443 Bacteria included in existing microfluidic models of bacterial infection at the vascular
444 interface are primarily common laboratory strains of prevalent pathogenic bacteria. Bacterial
445 species and strains vary significantly in their genotypes and phenotypes. For a more generalized
446 understanding of the vascular response to infection, models should incorporate additional
447 bacterial strains, including clinical isolates of bacteria. Current models have also been limited to
448 the study of the planktonic phenotype of bacteria. Bacterial infections are not always caused by
449 planktonic bacteria. The bacterial biofilm phenotype is a significant clinical problem as biofilms
450 are recalcitrant—resistant or tolerant—to antimicrobial treatment⁵⁴. Bacterial biofilms—
451 structured communities of cells encapsulated in self-produced matrix materials, including
452 polysaccharides, proteins, and DNA⁵⁵—are estimated to be involved in 65-80% of infections
453 annually⁵⁶. Biofilm formation can occur at the vascular interface during catheter-associated
454 infections, bloodstream infections, infective endocarditis, deep wound or surgical site infections,
455 and bacterial meningitis. There are not currently microfluidic models of biofilm infections at or
456 near the vascular interface. The inclusion of biofilms within microfluidic models requires
457 microfluidic model design that enables the co-culture of biofilms and mammalian cells on
458 relevant time scales. For biofilm development, bacteria will need to be included within the
459 microfluidic system for time periods of at least 24 hours and biofilm growth will need to be
460 optimized in environments that maintain the physiologically relevant properties of mammalian

461 cells within the model (e.g. mammalian culture media, physiological shear stress). Establishing
462 microfluidic models of biofilm development at the vascular interface will enable scientific
463 questions to be addressed, such as how the biofilm microenvironment and nutrient transport is
464 modulated by the vascular endothelium or how the vascular endothelium influences biofilm
465 recalcitrance to antimicrobial treatments. In addition to developing models of single species
466 biofilm communities in microphysiological systems, multispecies biofilms are also a prevalent
467 source of infection that exhibit behaviors that could be further understood utilizing microfluidic
468 models. Additionally, free-floating bacterial aggregates are emerging as an infection phenotype
469 ^{57, 58} that could be studied in these microfluidic systems.

470 Bacterial-derived molecules, such as LPS or fMLP, have been integrated into
471 microfluidic models to stimulate the inflammatory response of the vascular endothelium or the
472 recruitment of immune cells to an infection site. These are only two of many bacterial-derived
473 cues that are known to stimulate host responses. There are a variety of PAMPs produced by both
474 Gram-negative and Gram-positive pathogens that can trigger an inflammatory response from the
475 vascular endothelium ⁵⁹. Integrating multiple PAMPs or bacteria and specific PAMPs into
476 microfluidic models in a controlled manner will enable mechanistic studies of the specific roles
477 of PAMPs and bacteria in the pathogenesis of bacterial infections.

478 In addition to consideration of bacteria and bacterial-derived molecules within infection
479 models, the selection of the biological elements representative of the host is important to the
480 design of microfluidic models of bacterial infection. The use of cells with patient specificity
481 within microfluidic models of organ systems is a key consideration in device design ⁶⁰. Primary
482 cells or patient-derived stem cells could be used within microfluidic models to increase the
483 patient specificity of the microfluidic models for the endothelial cells, immune cells, or modeled

PLEASE CITE THIS ARTICLE AS DOI: 10.1063/5.0179281

484 organ tissue cells found within bacteria infection models. Additionally, immune cell response in
485 current models has focused on the initial recruitment of neutrophils or macrophage to an
486 infection site. However, the host immune response is not isolated to individual immune cells.
487 Vasculature-on-a-chip and organ-on-a-chip models provide a unique platform for isolating the
488 individual and cooperative responses of different immune cells to determine the role of cell-to-
489 cell communication between the vascular endothelium and bacteria in the host immune response
490 to infection. Host-derived cues of infection are also important to consider within models of
491 bacterial infection. When host cells are damaged or dying due to bacterial infections, they
492 release cues known as damage-associated molecular patterns (DAMPs) that signal the
493 inflammatory and innate immune response to infections⁶¹. Microfluidic bacterial infection
494 models that incorporate the vasculature are a promising platform for evaluating how isolated
495 DAMPs as well as the interactions between PAMPs and DAMPs influence the host response to
496 bacterial infections.

497 Recent advancements in vasculature-on-a-chip and vessel-on-a-chip device development
498 have recapitulated a variety of geometries and biological features that can be employed for
499 studying bacterial infections at the vascular interface. Device geometry has moved from two-
500 dimensional to rectangular to semi-circular to circular endothelial monolayers⁶². Biological
501 layers across the vessel wall including endothelial cells, the extracellular matrix, fibroblasts, and
502 smooth muscle cells have been incorporated into microfluidic models of the vasculature to better
503 represent physiological environments⁶². Stretchable and deformable vessels have been
504 engineered to enable the recapitulation of pulsatile blood flow in vessel-on-a-chip models⁶².
505 Additionally, microfluidic models of reversed flow due to bifurcations, sharp curves, or local
506 expansion of vessel geometry have been developed⁶². There are also vascular specific disease or

PLEASE CITE THIS ARTICLE AS DOI: 10.1063/5.0179281

507 injury states that may contribute to the recalcitrance of bacterial infections that have been
508 modeled using microfluidic devices, including vessel injury, endothelial dysfunction,
509 thrombosis, and vascular inflammation^{62, 63}. In addition to modifying device geometries and
510 biological features, bacterial infections in specific vascular microenvironments can be
511 recapitulated in future infection models, such as central venous catheter infections, intravenous
512 catheter infections, or infective endocarditis. Endothelial cell type and shear stress are two
513 critical components of the microenvironment that vary throughout the vasculature and are
514 important design considerations for developing site-specific infection models. Vessels in
515 microfluidic devices have been formed with aortic⁶⁴, microvascular⁶⁵, vein⁶⁶, and lymphatic⁶⁷
516 endothelial cells depending on the type of vessel being modeled. Shear stress within the vascular
517 system varies from 0.1 – 9.5 Pa, with lowest shear stresses in large capillary and large venous
518 vessels and highest shear stresses in small capillary and small arterial vessels^{68, 69, 70}. Shear
519 stress used within a microfluidic model can be modulated according the location, size, and health
520 of the vasculature being modeled⁷⁰. Existing vessel-on-a-chip models could be adapted to
521 represent specific infection sites by varying endothelial cell selection and shear stress within the
522 model. For example, a central venous catheter infection could be developed by including venous
523 endothelial cells and utilizing a shear stress of 0.35 Pa, which is the shear stress of a mid-sized
524 vein⁷¹, while an infective endocarditis model could be developed using valvular endothelial cells
525 and a shear stress of 2 Pa, which is the average shear stress at the aortic valve⁷². As discussed
526 here, there are many opportunities for existing microphysiological models of the healthy and
527 diseased vasculature to be adapted for studying bacterial infections at the vascular interface.
528 As was highlighted above in studies of bacterial infections in disease-on-a-chip models of
529 CF and COPD^{46, 53}, there are research opportunities available for studying how bacterial

530 infections progress in diseased or injured organs as diseased and injured tissue typically respond
531 differently to treatment than healthy tissue. Disease specific organ-on-a-chip models are rapidly
532 being developed across organ systems ⁷³. Microfluidic wound models inclusive of the
533 vasculature have been developed for studying wound healing and inflammation of injured tissue
534 ^{74, 75, 76}. However, microfluidic models of wound infections inclusive of the vasculature are yet
535 to be utilized for studying bacterial infections. This is an important direction of research as
536 injured tissue, such as the tissue in chronic wounds and burns, has an increased susceptibility to
537 bacterial infection ^{77, 78}. Future research opportunities in infectious disease research utilizing
538 wound-on-a-chip models include evaluation of host-pathogen interactions, the influence of
539 bacteria on wound closure and healing, and the progression of bacterial infections in deep
540 wounds, chronic wounds, and surgical incision sites. As more disease and injury specific-organ
541 models emerge, bacterial infections within these models can be investigated and a mechanistic
542 understanding of why bacterial infections are more difficult to treat for patients with specific
543 diseases and injuries can be revealed.

544 In addition to the utilization of organ-on-a-chip models for studying bacterial infections,
545 there are parallel research efforts in utilizing organ-on-a-chip models for studying viral
546 infections, as reviewed elsewhere ^{35, 36, 79, 80, 81}. Microfluidic viral infection models inclusive of
547 the vasculature have been developed using lung-on-a-chip models ^{82, 83}, a skin-on-a-chip model
548 ⁸⁴, and a liver-on-a-chip model ⁸⁵; these microphysiological systems have been used to study
549 viral pathogenesis, host immune response, and antiviral efficacy. The approaches and methods
550 used to study viral infections in organ-on-a-chip models can be adapted for informing the
551 development of bacterial infection models and vice versa, especially when infection models have
552 only been developed using one class of infectious agent. For example, Nawroth et al. developed

553 an airway lung chip inclusive of vascular endothelial cells and neutrophils to probe mechanisms
554 leading to human rhinovirus (HRV)-induced asthma exacerbation⁸³. Bacteria, including
555 *Streptococcus pneumoniae*, *Hemophilus influenza*, and *Moraxella catarrhalis*, are also known to
556 exacerbate asthma⁸⁶. Therefore, Nawroth et al.'s airway lung chip modeling HRV-induced
557 asthma exacerbation⁸³ could be adapted for the study of bacterial-induced asthma exacerbation.
558 Similarly, Sun et al.'s vascularized skin-on-a-chip model of a herpes simplex virus (HSV)
559 infection that replicated host inflammatory and immune responses to HSV ulcerations⁸⁴ could be
560 adapted for studying bacterial infections of skin lesions, such as ulcers or wounds. Thus,
561 microfluidic models of viral infections can be utilized to inspire the future development of
562 bacterial infection models.

563 Multi-organ-on-a-chip and body-on-a-chip microphysiological systems are being
564 developed to enable systemic studies of interactions and crosstalk between organs using
565 physiologically relevant *in vitro* models^{60, 87, 88}. In one such multi-organ chip model inclusive of
566 vasculature, heart, liver, bone, and skin tissues are connected by vasculature with recirculating
567 flow⁸⁹. This multi-organ-on-a-chip model showed improved predictive values of cardiotoxicity
568 biomarkers relative to isolated tissues. There is immense potential for exploiting body-on-a-chip
569 models to investigate the systemic response of the host to bacterial infections during specific
570 disease states, such as sepsis, bloodstream infections, or the spread of secondary infections as
571 well as in evaluating the efficacy of innovative antimicrobial treatments.

572 The rise of antimicrobial resistance in bacterial strains demands new antimicrobials and
573 approaches for treating bacterial infections. Predictions estimate that by 2050 up to 10 million
574 deaths may be attributed to antimicrobial resistance annually⁹⁰. Vasculature-on-a-chip and
575 organ-on-a-chip models inclusive of vasculature can be applied in the development of innovative

576 antimicrobial solutions for treating bacterial infections. The efficacy of antimicrobial agents and
577 biomaterials can be tested using microphysiological models ⁶⁰. This is exemplified by the
578 previously highlighted urinary tract infection model, which observed intracellular bacterial
579 communities contribute to the dynamic persistence of infection during antibiotic treatment ⁴¹.
580 Additionally, emerging therapeutic targets for preserving or restoring vascular function after
581 degradation due to bacterial sepsis, such as therapeutic interventions to restore the endothelial
582 glycocalyx ⁹¹, can be evaluated in these model systems. The devices can also be modified to
583 include patient-specific bacteria or patient-derived cells for personalized evaluation of
584 antimicrobial solutions in microfluidic systems ⁷³. Finally, scale-up of the microfluidic models
585 will be required to enable high-throughput approaches for pre-clinical predication of
586 antimicrobial effectiveness, which would reduce cost, amount of time, and number of animal
587 models used in antimicrobial development.

588

589 **6. Conclusions**

590 This review considers microfluidic technologies for studying bacterial infections at or
591 near the vascular interface. Current microfluidic models of bacteria and bacterial-derived
592 molecules at or near the vascular interface have enabled studies of the inflammatory response of
593 the vasculature as well as the initial host immune response to bacterial infections. Existing
594 models contain a limited number of pathogenic bacteria, bacterial-derived molecules, and host
595 cells. Extending current models to include different biological elements will provide new
596 insights into how bacterial infections progress at and near the vasculature. The latest
597 technological developments in vasculature-on-a-chip, organ-on-a-chip, and body-on-a-chip
598 models provide numerous opportunities for advancing the understanding of bacterial interactions

599 with the vasculature during infections. In addition, studying bacterial infections using disease-
600 on-a-chip models will enable newfound understanding of why bacterial infections are more
601 prevalent in certain disease states. Current models can also be modified for the development and
602 testing of novel antimicrobial treatments for bacterial infections. Furthermore, the use of patient-
603 derived bacteria, vascular cells, or immune cells within microfluidic models could enable the
604 development of personalized antimicrobial treatments. Overall, technological advancements in
605 the microfabrication of microfluidic systems inclusive of the vasculature have led to measurable
606 advances in the understanding of how bacteria and bacterial-derived molecules inform the host
607 response to infection. Emerging microfluidic technologies offer additional promise for
608 transforming the scientific understanding of bacterial pathogenesis and supporting the
609 development of innovative antimicrobial solutions in the future.

610

611 **Acknowledgements**

612 This work was supported by the National Science Foundation (Grant CBET-2301586) and
613 Worcester Polytechnic Institute. All figures in this review were created with BioRender.com.

614

615 **Author Contributions Statement**

616 **Lily Isabelle Gaudreau:** Conceptualization (supporting); Visualization (lead); Writing- original
617 draft (equal); Writing- review & editing (equal). **Elizabeth J. Stewart:** Conceptualization
618 (lead); Visualization (supporting); Writing- original draft (equal); Writing- review & editing
619 (equal); Project Administration (lead); Supervision (lead); Funding Acquisition (lead).

620

621 **Conflict of Interest Statement**

622 The authors declare no competing financial interests.

623

624 **Data Availability Statement**

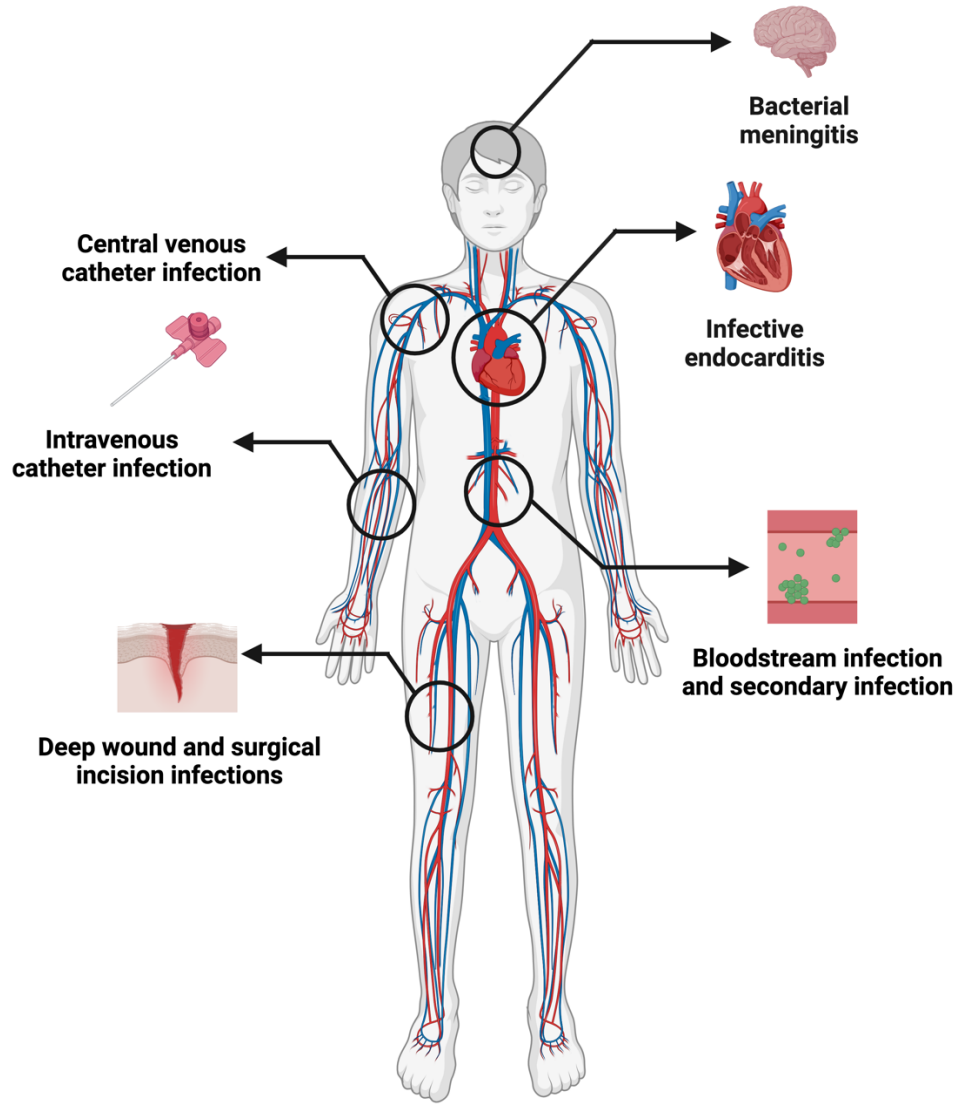
625 Data sharing is not applicable to this article as no new data were created or analyzed in this

626 study.

627

628 **Figures**

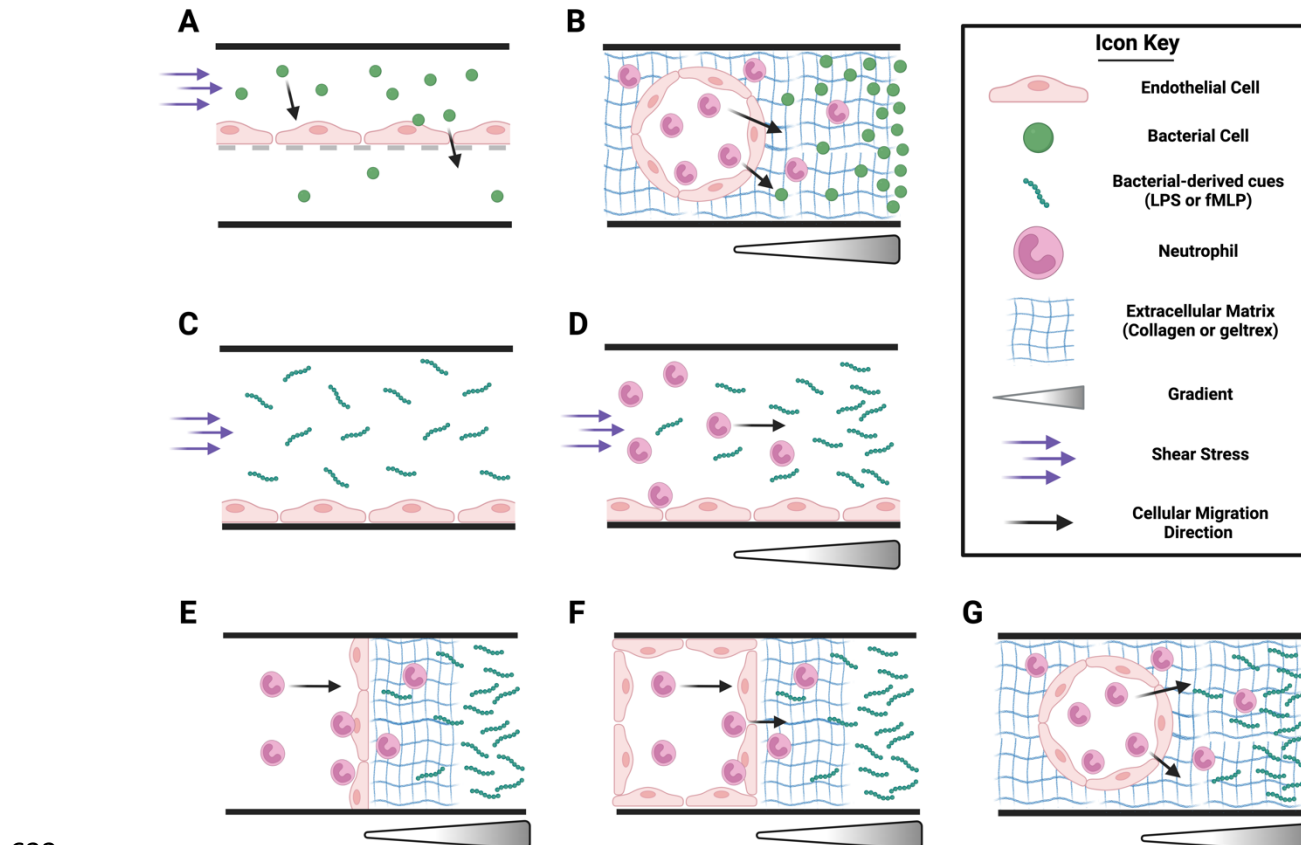
PLEASE CITE THIS ARTICLE AS DOI: 10.1063/5.0179281



629

630 **Figure 1. Bacterial infections that occur at the vascular interface throughout the body.**631 Schematic indicating the various locations and types of infections where bacteria directly interact
632 with the vasculature.

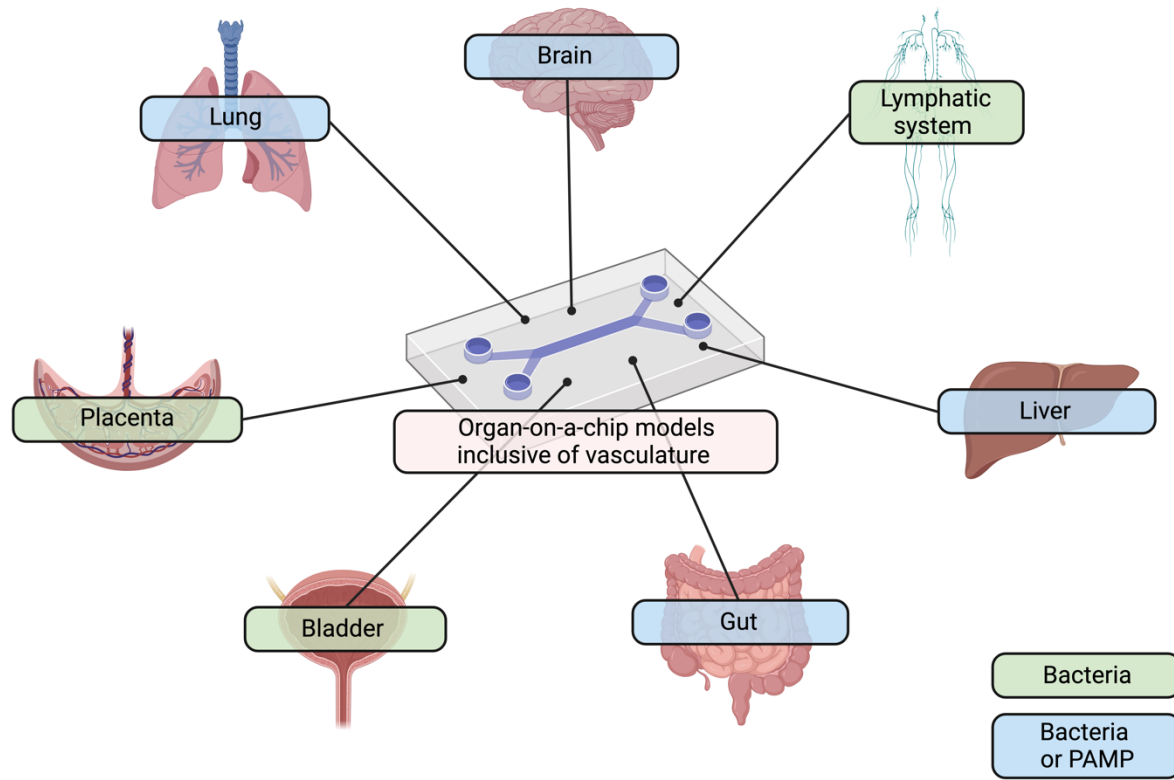
PLEASE CITE THIS ARTICLE AS DOI: 10.1063/5.0179281



633

634 **Figure 2. Vasculature-on-a-chip models inclusive of bacteria and bacterial-derived**
635 **molecules.** Vasculature-on-a-chip devices that include intact bacteria have modeled (A) bacterial
636 extravasation from the blood stream via transendothelial migration across a 2D endothelial
637 monolayer and (B) neutrophil transendothelial migration from a 3D cylindrical vessel through
638 ECM toward intact bacteria. In addition, microfluidic models of the vasculature have modeled
639 endothelial response to bacterial-derived cues in the bloodstream (C) without and (D) with
640 neutrophils. Microfluidic systems have also modeled neutrophil transendothelial migration
641 toward bacterial-derived cues located in the host tissue by including the ECM in the model with
642 endothelial geometries varying in complexity from (E) a 2D monolayer to (F) a 3D rectangular
643 vessel to (G) a 3D cylindrical vessel. Shear stress in models depicted in 2B, 2E, 2F, and 2G is
644 perpendicular to the plane of view.

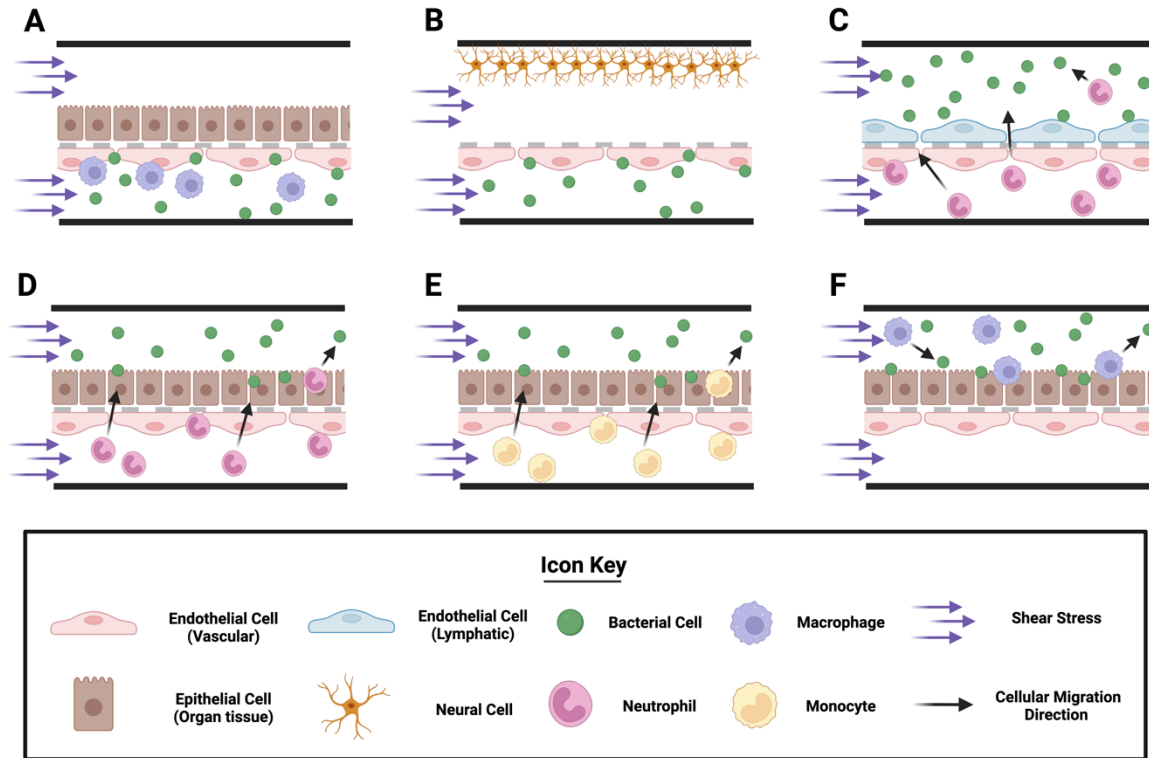
PLEASE CITE THIS ARTICLE AS DOI: 10.1063/5.0179281



645

646 **Figure 3. Organs represented in organ-on-a-chip models inclusive of vasculature and**
647 **bacterial infections.** Bacterial infections in the lung, brain, lymphatic system, liver, gut,
648 bladder, and placenta have been modeled in organ-on-a-chip devices inclusive of the vasculature.
649 Organ labels shaded in green have investigated intact bacteria in the models. Organ labels
650 shaded in blue have included intact bacteria or a PAMP in the model.

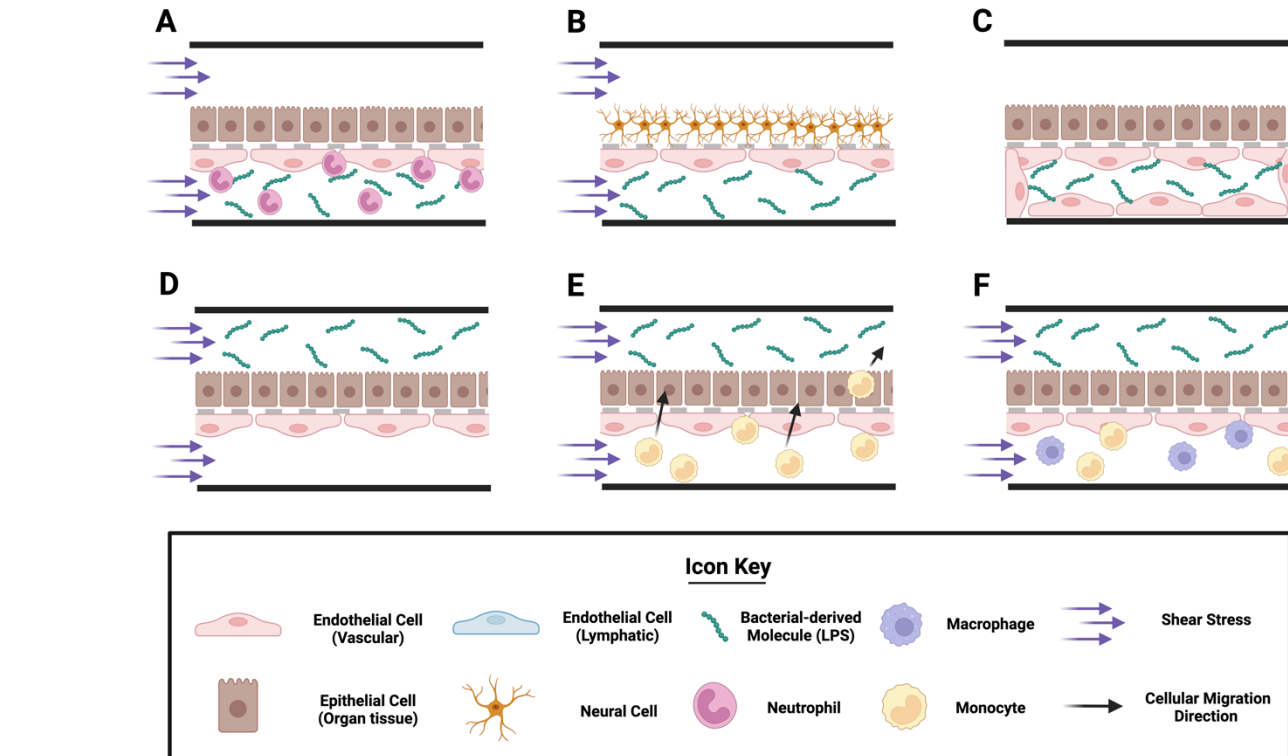
PLEASE CITE THIS ARTICLE AS DOI: 10.1063/5.0179281



651

652 **Figure 4. Organ-on-a-chip models inclusive of vasculature and bacteria representing either**
653 **bloodstream or organ infections.** Organ-on-a-chip systems that included intact bacteria in the
654 bloodstream have modeled: (A) macrophage response to bacteria in a blood vessel adjacent to
655 the liver and (B) bacterial infections at the blood-brain interface. Organ-on-a-chip systems that
656 included intact bacteria within organ tissues have modeled: (C) neutrophil transendothelial
657 migration from the bloodstream to a lymphatic vessel containing intact bacteria, (D) neutrophil
658 transendothelial migration from the bloodstream towards a lung or bladder infection, (E)
659 monocyte transendothelial migration from the bloodstream to a lung infection, and (F)
660 macrophage response to bacterial infections in the lung or placenta.

PLEASE CITE THIS ARTICLE AS DOI: 10.1063/5.0179281



661

662 **Figure 5. Organ-on-a-chip models inclusive of vasculature and bacterial-derived molecules.**

663 Organ-on-a-chip systems that include the bacterial-derived molecule lipopolysaccharide (LPS) in
664 the bloodstream have modeled: (A) neutrophils and LPS in a blood vessel adjacent to the liver,
665 (B) LPS in the bloodstream at the blood-brain barrier, and (C) LPS in a 3D blood vessel adjacent
666 to the lung. Organ-on-a-chip systems that included LPS within the host tissue have modeled: (D)
667 LPS in the lung, (E) monocyte transendothelial migration from the bloodstream to LPS in the
668 liver, and (F) the response of monocytes and macrophage in the bloodstream to LPS in the gut.
669 Shear stress in the model depicted in 2C is perpendicular to the plane of view.

670 **Tables**671 **Table 1.** Vasculature-on-a-chip models used to study the vascular response to bacterial infection.

Pathogen	Biological Process	Device Design	Key Scientific Findings	Ref.
<i>Borrelia burgdorferi</i>	Bacterial extravasation out of the bloodstream	Device Design: Two channels separated by a PET membrane with 3 μ m pores in a microfluidic device that mimicked a transwell dish Endothelium Geometry: 2D ECM: No	Bacterial transendothelial migration while undergoing shear stress is initially delayed compared to static conditions, but after \sim 1 hour bacterial migration rates become similar under shear and static conditions.	²⁰
<i>Pseudomonas aeruginosa</i>	Neutrophil migration from the blood vessel toward bacteria	Device Design: Large PDMS chamber filled with a collagen hydrogel containing a suspended cylindrical channel lined with endothelial cells Endothelium Geometry: 3D, cylindrical vessel ECM: Yes, collagen	An endothelial monolayer is needed for persistent neutrophil migration out of the vessel into the ECM toward intact bacteria. Neutrophil migration time toward infection was much longer than expected (up to 24 hours).	²¹

672 **Abbreviations:** Polyethylene terephthalate (PET); Polydimethylsiloxane (PDMS); Extracellular matrix (ECM)

673 **Table 2.** Vasculature-on-a-chip microfluidic models used to study the vascular response to
 674 bacterial-derived molecules.

Bacterial-Derived Molecule	Biological Process	Device Design	Key Scientific Findings	Ref.
LPS	Vascular inflammation and monocyte transendothelial migration	Device Design: PDMS chip with three channels for endothelial cells, a hydrogel, and media with LPS to create a concentration gradient across the hydrogel. Endothelium Geometry: 3D rectangular vessel ECM: Yes, collagen I	- ICAM-1 expression increased 136% and 289% and VE-cadherin expression decreased 43% and 37% after 4 and 8 hours of LPS treatment, respectively. - The number of adhered and transmigrated monocytes increased 57% and the distance migrated into the ECM increased by 95% with LPS treatment.	²⁴
LPS	Endothelial glycocalyx degradation	Device Design: PDMS flow cell. Endothelium Geometry: 2D ECM: No	- LPS treatment activates endogenous enzyme, HSPE1, which causes glycocalyx shedding and signals the production of the inflammatory cytokine IL-6 - Overexpression of endogenous inhibitor HPSE2 downregulated inflammatory pathways within endothelial cells and protected the vascular endothelium from endothelial glycocalyx shedding due to LPS.	²⁶
LPS	Endothelial glycocalyx degradation	Device Design: PDMS chip with single rectangular channel or branched channel network. Endothelium Geometry: 2D ECM: No	- Glycocalyx and VE-cadherin expression decreased by 18% and 22%, respectively, due to LPS treatment. - DEX inhibited glycocalyx degradation and VE-cadherin expression induced by LPS.	²⁷
fMLP	Neutrophil migration	Device Design: PDMS chip with serpentine channels for generating a chemoattractant gradient that interfaces with a large rectangular observation channel. Endothelium Geometry: 2D ECM: No	- Neutrophils preferentially migrate toward fMLP with and without a competing chemoattract gradient, showing prioritization of chemotaxis toward fMLP.	²⁸
fMLP	Neutrophil adhesion and transendothelial migration	Device Design: PDMS chip with a physiological microvascular channel network and channels with three parallel compartments. Endothelium Geometry: 3D, semi-circular vessels ECM: No	- Neutrophil migration across an activated endothelium toward fMLP was inhibited 85-92% after treatment with protein kinase C δ (PKC δ). - The number of neutrophils adhered to an activated endothelium decreased by 46% after treatment with PKC δ .	²⁹
fMLP	Neutrophil transendothelial migration	Device Design: PDMS chip with five rectangular channels that enable measurements of chemoattractant driven neutrophil transendothelial migration and ECM migration Endothelium Geometry: 3D, rectangular vessel ECM: Yes, collagen	- An endothelial monolayer was required for neutrophil transendothelial migration toward fMLP into a collagen ECM as there was negligible neutrophil migration into the ECM without an endothelial monolayer. - Lower collagen ECM stiffness increased the speed and distance of neutrophil migration under optimal fMLP concentrations.	³⁰
fMLP	Neutrophil transendothelial migration	Device Design: Upper chamber with endothelial cells and lower ECM chamber with varied curvatures and bifurcations. Endothelium Geometry: 3D, rectangular vessel ECM: Yes, collagen	- Neutrophil transendothelial migration within a hydrogel was \sim 600% greater with fMLP present.	³²
fMLP	Neutrophil transendothelial migration	Device Design: PDMS chip with two side channels, one bottom channel, and a central gel chamber where cells are cultured against a hydrogel.	- High concentrations of chemoattractants induce steep chemoattractant gradients that result in significant neutrophil transendothelial migration. - Multiple chemoattractants show synergistic effects in neutrophil transendothelial migration.	³¹

		Endothelium Geometry: 2D, vertical plane ECM: Yes, collagen I	- Neutrophils do not migrate into the collagen hydrogel without endothelial cells within the device.	
fMLP	Neutrophil transendothelial migration	Device Design: PDMS chamber with a cylindrical channel lined with endothelium derived from iPSCs suspended in a collagen hydrogel. Endothelium Geometry: 3D, cylindrical vessel ECM: Yes, collagen	- Neutrophil transendothelial migration toward fMLP was stronger from whole blood than from purified neutrophils.	³³
fMLP	Endothelial inflammation and neutrophil transendothelial migration	Device Design: Three adjacent channels separated by Phaseguides to enable endothelial vessels to grow in direct contact with ECM. Endothelium Geometry: 3D, rectangular vessel ECM: Yes, collagen I and geltrex	- Neutrophils migrated through geltrex without fMLP but were unable to migrate into collagen I ECM without the presence of endothelial cells and fMLP stimulation. - Neutrophils readily migrated across a geltrex ECM toward fMLP, but 58% fewer neutrophils migrated into a collagen I ECM toward fMLP with some neutrophils stalling within the ECM.	³⁴

675 **Abbreviations:** Polydimethylsiloxane (PDMS); Extracellular matrix (ECM); Lipopolysaccharides (LPS); N-formyl-
 676 methionyl-leucyl-phenylalanine (fMLP); Endo- β -D-glucuronidase heparanase-1 (HPSE1); HPSE1 inhibitor
 677 heparanase-2 (HPSE2); Dexmedetomidine (DEX); Induced pluripotent stem cells (iPSCs); Intercellular adhesion
 678 molecule-1 (ICAM-1); Vascular endothelial cadherin (VE-cadherin)

679 **Table 3.** Organ-on-a-chip microfluidic models used to study vascular and host tissue responses
 680 to bacterial infections.

Model and Cell Types	Device Design	Pathogen & Infection Site	Immune Cell (Y/N; type; location)	Vascular and Immune Responses to Infection	Ref.
Model: Lung Mammalian Cells: <ul style="list-style-type: none">- Human alveolar epithelial cells- Human pulmonary microvascular endothelial cells	- PDMS chip with two channels separated by a flexible membrane with 10 μm pores <ul style="list-style-type: none">- Vacuum channels utilized to recapitulate deformation during respiration	Bacteria: <i>Escherichia coli</i> Infection Site: Host tissue (epithelial channel)	Yes - Neutrophils; Bloodstream (endothelial channel)	- Endothelium captures circulating neutrophils indicative of an increase in endothelial ICAM-1 expression during infection. <ul style="list-style-type: none">- Neutrophils transmigrate from the endothelial channel into alveolar chamber with directed movement toward bacteria.Neutrophils then clear bacteria via engulfment.	³⁹
Model: Lymphatic System Mammalian Cells: <ul style="list-style-type: none">- Lymphatic endothelial cells (HLECs)- Human Umbilical Vein Endothelial Cells (HUVECs)	- Large PDMS chamber filled with collagen or fibronectin hydrogel in which a cylindrical channel is cast and lined with endothelial cells (LumeNEXT device)	Bacteria: <i>Pseudomonas aeruginosa</i> Infection Site: Lymphatic System (Lymphatic endothelial channel)	Yes - Neutrophils; Bloodstream (vascular endothelial channel)	- Bacterial infection resulted in increased endothelial expression of the proinflammatory cytokines IL-1 α and IL-6 as well as the anti-inflammatory cytokine IL-10. <ul style="list-style-type: none">- Lymphatic endothelial (LECs) vessels increase neutrophil migration to bacteria by 157%, but presence of both HUVEC and LECs vessels results in only a 27% increase, indicating cross talk between the vessels.	⁴⁰
Model: Bladder Mammalian Cells: <ul style="list-style-type: none">- Bladder epithelial cells- Bladder microvascular endothelial cells	- PDMS chip with two rectangular channels separated by a stretchable porous membrane <ul style="list-style-type: none">- Negative pressure used to induce strain on the membrane, simulating bladder filling and voiding	Bacteria: Uropathogenic <i>Escherichia coli</i> (UPEC) Infection Site: Host tissue (epithelial channel)	Yes - Neutrophils; Bloodstream (endothelial channel)	- Increased expression of ICAM-1 on endothelial cells enabled for robust neutrophil attachment to endothelial layer and mediated diapedesis of neutrophils during bacterial infection. <ul style="list-style-type: none">- UPEC infection model creates a strong proinflammatory cytokine gradient of IL-1α, IL-1β, IL-6, and IL-8 to drive neutrophil recruitment.	⁴¹
Model: Liver Mammalian Cells: <ul style="list-style-type: none">- Liver epithelial cells- Human Umbilical Vein Endothelial Cells (HUVECs)	-PDMS chip with two rectangular microfluidic channels separated by a thin membrane with 8 μm pores	Bacteria: Methicillin resistant <i>Staphylococcus aureus</i> Infection Site: Bloodstream (endothelial channel)	Yes - Macrophages; Bloodstream (endothelial channel)	- Macrophages increase the concentrations of IL-1 β , IL-18, IL-6, and IL-10 proinflammatory cytokines within liver-on-a-chip model.	⁴²
Model: Lung Mammalian Cells: <ul style="list-style-type: none">- Lung epithelial cells (NCI-H441)- Human Umbilical Vein Endothelial Cells (HUVECs)	-PDMS chip with two channels separated by a membrane with 8 μm pores	Bacteria: <i>Staphylococcus aureus</i> (with influenza virus) Infection Site: Host tissue (epithelial channel)	Yes – Macrophages; Host tissue (epithelial channel)	- Coinfection of bacteria and a virus led to a significant reduction of VE-cadherin expression and a disrupted endothelial barrier that enabled bacteria to translocate from the lung epithelial channel to the endothelial channel.	⁴³
Model: Placenta Mammalian Cells: <ul style="list-style-type: none">- Trophoblasts (placental epithelial cells)- Human Umbilical Vein Endothelial Cells (HUVECs)	-PDMS chip with two rectangular channels separated by a semipermeable membrane with 0.4 μm pores	Bacteria: <i>Escherichia coli</i> Infection Site: Host tissue (epithelial channel)	Yes – Macrophages; Host tissue (epithelial chamber)	- The vascular endothelium has a loss of VE-cadherin, barrier integrity, and some cell death via apoptosis during a bacterial infection. <ul style="list-style-type: none">- Bacteria also increased the production of proinflammatory cytokines IL-1α, IL-1β, IL-6, IL-8 in the placenta-on-a-chip model.	⁴⁴

Model: Brain Mammalian Cells: - Neuronal hippocampal cells - Human Umbilical Vein Endothelial Cells (HUVECs)	- Transwell platform with a 3D printed insert chip - 3D printed insert chip is made of a clear resin with a porous membrane as the base	Bacteria: <i>Escherichia coli</i> Infection Site: Bloodstream (endothelial channel)	No	- Bacterial infection resulted in decreased VE-cadherin expression and increased permeability of the endothelium as well as increased expression of the proinflammatory cytokine IL-6 expression and von Willebrand Factor by the endothelial cells.	45
Model: Lung Mammalian Cells: - Cystic Fibrosis bronchial epithelial cells - Pulmonary microvascular endothelial cells	-PDMS chip with two parallel, linear channels separated by a membrane with 7 μ m pores	Bacteria: <i>Pseudomonas aeruginosa</i> Infection Site: Host tissue (epithelial channel)	Yes - Polymorphonuclear leukocytes (PMNs); Bloodstream (endothelial channel)	- Bacterial infection in a CF model showed increases in PMN adhesion to the endothelium, but no increase in the transmigration of PMNs. - Bacterial infection increased endothelial expression of the proinflammatory cytokine IL-6.	46

681 **Abbreviations:** Polydimethylsiloxane (PDMS); Intercellular adhesion molecule-1 (ICAM-1); Vascular endothelial

682 cadherin (VE-cadherin)

683 **Table 4.** Organ-on-a-chip microfluidic models used to study the vascular and host responses to
 684 bacterial-derived molecules.

Model and Cell Types	Device Design	PAMP & Infection Site	Immune Cell (Y/N; type; location)	Vascular and Immune Responses to Infection	Ref.
Model: Liver Mammalian Cells: - Murine hepatic epithelial cells - Liver sinusoidal endothelial cells - Kupffer cells	- PDMS chip with two rectangular channels separated by a membrane with 0.4 μ m pores	PAMP: LPS Infection Site: Bloodstream (endothelial channel)	Yes - Neutrophils; Bloodstream (endothelial channel)	- LPS treatment resulted in increased neutrophil adherence to the endothelium and increased neutrophil aggregate size.	⁴⁷
Model: Gut Mammalian Cells: - Intestinal epithelial cells - Lymphatic microvascular endothelial cells	- PDMS chip with two rectangular channels separated by a thin membrane with 10 μ m pores - Pneumatics used to apply cyclic strain to cell culture chamber	PAMP: LPS Infection Site: Host tissue (epithelial channel)	Yes - Monocytes and Macrophages; Bloodstream (endothelial channel)	- Treatment with LPS, monocytes, and macrophage resulted in increased ICAM-1 expression on endothelium surface.	⁴⁹
Model: Liver Mammalian Cells: - Hepatocytes, liver epithelial cells - Human Umbilical Vein Endothelial Cells (HUVECs)	- MOTiF biochip made from polystyrol with two chambers separated by a membrane with 8 μ m pores	PAMP: LPS Infection Site: Host tissue (epithelial chamber)	Yes - Monocytes; Bloodstream (endothelial chamber)	- LPS treatment resulted in monocyte recruitment to the endothelium and transendothelial migration of monocytes to the hepatic compartment. - LPS treatment reduces endothelial barrier integrity as evidenced by loss of VE-cadherin and ZO-1.	⁵⁰
Model: Brain Mammalian Cells: - Human astrocytes - Human Umbilical Vein Endothelial Cells (HUVECs)	-PDMS chip with two channels separated by a polycarbonate membrane with 0.4 μ m pores	PAMP: LPS Infection Site: Bloodstream (endothelial channel)	No	- LPS treatment reduced barrier integrity of vasculature as shown by the discontinuous distribution of tight junction protein, ZO-1, throughout the endothelium after 12 hours of LPS treatment and reduced expression of ZO-1 over time.	⁵¹
Model: Lung Mammalian Cells: - Alveolar epithelial cells - Human Umbilical Vein Endothelial Cells (HUVECs)	-PDMS chip with two parallel rectangular microchannels separated by a thin membrane	PAMP: LPS Infection Site: Host tissue or Bloodstream (epithelial or endothelial channel)	No	- LPS treatment of alveolar epithelial channel resulted in ~5.5x increase in tissue-tissue permeability, but not when LPS was added to the endothelial channel. - LPS treatment increased endothelial expression of ICAM-1 and proinflammatory cytokine expression of IL-6, IL-8, and MCP1.	⁵²
Model: Lung Mammalian Cells: - Human alveolar epithelial cells - Primary human lung microvascular endothelial cells	-PDMS with two rectangular channels separated by a membrane with 0.4 μ m pores	PAMP: LPS Infection Site: Host tissue (epithelial channel)	No	- LPS treatment increased endothelial expression of proinflammatory cytokine IL-8 and macrophage stimulating factor (M-CSF) in COPD model as compared to a healthy lung model.	⁵³

685 **Abbreviations:** Polydimethylsiloxane (PDMS); Pathogen-associated Molecular Pattern (PAMP);
 686 Lipopolysaccharides (LPS); Intercellular adhesion molecule-1 (ICAM-1); Vascular endothelial cadherin (VE-
 687 cadherin); Zonula occludens tight junction protein-1 (ZO-1); Chronic obstructive pulmonary disease (COPD)

688 **References**

689 ¹ M.K. Pugsley, and R. Tabrizchi, "The vascular system: An overview of structure and function,"
690 *J. Pharmacol. Toxicol. Methods* **44**(2), 333–340 (2000).

691 ² E. Lemichez, M. Lecuit, X. Nassif, and S. Bourdoulous, "Breaking the wall: targeting of the
692 endothelium by pathogenic bacteria," *Nat. Rev. Microbiol.* **8**(2), 93–104 (2010).

693 ³ R.R. Isberg, and P. Barnes, "Dancing with the Host: Flow-Dependent Bacterial Adhesion," *Cell*
694 **110**(1), 1–4 (2002).

695 ⁴ M. Phillipson, and P. Kubes, "The neutrophil in vascular inflammation," *Nat. Med.* **17**(11),
696 1381–1390 (2011).

697 ⁵ S. Denk, M. Perl, and M. Huber-Lang, "Damage- and Pathogen-Associated Molecular Patterns
698 and Alarmins: Keys to Sepsis?," *Eur. Surg. Res.* **48**(4), 171–179 (2012).

699 ⁶ J.W. Krueger, D.F. Young, and N.R. Cholvin, "An *in vitro* study of flow response by cells," *J.*
700 *Biomech.* **4**(1), 31–36 (1971).

701 ⁷ M.J. Levesque, and R.M. Nerem, "The elongation and orientation of cultured endothelial cells
702 in response to shear stress," *J. Biomech. Eng.* **107**(4), 341–347 (1985).

703 ⁸ A. Reinitz, J. DeStefano, M. Ye, A.D. Wong, and P.C. Searson, "Human brain microvascular
704 endothelial cells resist elongation due to shear stress," *Microvasc. Res.* **99**, 8–18 (2015).

705 ⁹ J.M. Tarbell, "Shear stress and the endothelial transport barrier," *Cardiovasc. Res.* **87**(2), 320–
706 330 (2010).

707 ¹⁰ K. Reddy, and J.M. Ross, "Shear Stress Prevents Fibronectin Binding Protein-Mediated
708 *Staphylococcus aureus* Adhesion to Resting Endothelial Cells," *Infect. Immun.* **69**(5), 3472–
709 3475 (2001).

710 ¹¹ K.D. Viegas, S.S. Dol, M.M. Salek, R.D. Shepherd, R.M. Martinuzzi, and K.D. Rinker,
711 “Methicillin resistant *Staphylococcus aureus* adhesion to human umbilical vein endothelial cells
712 demonstrates wall shear stress dependent behaviour,” *Biomed. Eng. OnLine* **10**(1), 20 (2011).

713 ¹² J. Claes, L. Liesenborghs, M. Peetermans, T.R. Veloso, D. Missiakas, O. Schneewind, S.
714 Mancini, J.M. Entenza, M.F. Hoylaerts, R. Heying, P. Verhamme, and T. Vanassche, “Clumping
715 factor A, von Willebrand factor-binding protein and von Willebrand factor anchor
716 *Staphylococcus aureus* to the vessel wall,” *J. Thromb. Haemost.* **15**(5), 1009–1019 (2017).

717 ¹³ K.I. Pappelbaum, C. Gorzelanny, S. Grässle, J. Suckau, M.W. Laschke, M. Bischoff, C. Bauer,
718 M. Schorpp-Kistner, C. Weidenmaier, R. Schneppenheim, T. Obser, B. Sinha, and S.W.
719 Schneider, “Ultralarge von Willebrand Factor Fibers Mediate Luminal *Staphylococcus aureus*
720 Adhesion to an Intact Endothelial Cell Layer Under Shear Stress,” *Circulation* **128**(1), 50–59
721 (2013).

722 ¹⁴ J.M. Kwiecinski, H.A. Crosby, C. Valotteau, J.A. Hippensteel, M.K. Nayak, A.K. Chauhan,
723 E.P. Schmidt, Y.F. Dufrêne, and A.R. Horswill, “*Staphylococcus aureus* adhesion in
724 endovascular infections is controlled by the ArlRS–MgrA signaling cascade,” *PLOS Pathog.*
725 **15**(5), e1007800 (2019).

726 ¹⁵ H. Jagau, I.-K. Behrens, K. Lahme, G. Lorz, R.W. Köster, R. Schneppenheim, T. Obser, M.A.
727 Brehm, G. König, T.P. Kohler, M. Rohde, R. Frank, W. Tegge, M. Fulde, S. Hammerschmidt,
728 M. Steinert, and S. Bergmann, “Von Willebrand Factor Mediates Pneumococcal Aggregation
729 and Adhesion in Blood Flow,” *Front. Microbiol.* **10**, 511 (2019).

730 ¹⁶ E. Mairey, A. Genovesio, E. Donnadieu, C. Bernard, F. Jaubert, E. Pinard, J. Seylaz, J.-C.
731 Olivo-Marin, X. Nassif, and G. Duménil, “Cerebral microcirculation shear stress levels

PLEASE CITE THIS ARTICLE AS DOI: 10.1063/5.0179281

732 determine *Neisseria meningitidis* attachment sites along the blood–brain barrier,” *J. Exp. Med.*
733 **203**(8), 1939–1950 (2006).

734 ¹⁷ Y. Zeng, Y. Qiao, Y. Zhang, X. Liu, Y. Wang, and J. Hu, “Effects of fluid shear stress on
735 apoptosis of cultured human umbilical vein endothelial cells induced by LPS,” *Cell Biol. Int.*
736 **29**(11), 932–935 (2005).

737 ¹⁸ A. Ploppa, V. Schmidt, A. Hientz, J. Reutershan, H.A. Haeberle, and B. Nohé, “Mechanisms
738 of leukocyte distribution during sepsis: an experimental study on the interdependence of cell
739 activation, shear stress and endothelial injury,” *Crit. Care* **14**(6), R201 (2010).

740 ¹⁹ M.E. Fallon, R. Mathews, and M.T. Hinds, “*In Vitro* Flow Chamber Design for the Study of
741 Endothelial Cell (Patho)Physiology,” *J. Biomech. Eng.* **144**(020801), (2021).

742 ²⁰ M. d Bergevin, A.E. Boczula, L. Caruso, H. Persson, C.A. Simmons, and T.J. Moriarty, “A
743 Live Cell Imaging Microfluidic Model for Studying Extravasation of Bloodborne Bacterial
744 Pathogens,” *Cell. Microbiol.* **2022**, e3130361 (2022).

745 ²¹ L.E. Hind, P.N. Ingram, D.J. Beebe, and A. Huttenlocher, “Interaction with an endothelial
746 lumen increases neutrophil lifetime and motility in response to *P. aeruginosa*,” *Blood* **132**(17),
747 1818–1828 (2018).

748 ²² D. Heumann, and T. Roger, “Initial responses to endotoxins and Gram-negative bacteria,”
749 *Clin. Chim. Acta* **323**(1), 59–72 (2002).

750 ²³ P.A. Ward, I.H. Lepow, and L.J. Newman, “Bacterial factors chemotactic for
751 polymorphonuclear leukocytes.,” *Am. J. Pathol.* **52**(4), 725–736 (1968).

752 ²⁴ U. Nam, S. Kim, J. Park, and J.S. Jeon, “Lipopolysaccharide-Induced Vascular Inflammation
753 Model on Microfluidic Chip,” *Micromachines* **11**(8), 747 (2020).

PLEASE CITE THIS ARTICLE AS DOI: 10.1063/5.0179281

754 ²⁵ F.E. Curry, and R.H. Adamson, “Endothelial Glycocalyx: Permeability Barrier and
755 Mechanosensor,” *Ann. Biomed. Eng.* **40**(4), 828–839 (2012).

756 ²⁶ Y. Kiyan, S. Tkachuk, K. Kurselis, N. Shushakova, K. Stahl, D. Dawodu, R. Kiyan, B.
757 Chichkov, and H. Haller, “Heparanase-2 protects from LPS-mediated endothelial injury by
758 inhibiting TLR4 signalling,” *Sci. Rep.* **9**(1), 13591 (2019).

759 ²⁷ W. Liao, L. Yi, W. He, S. Yang, P. Zhang, T. Weng, and Y. Xu, “A PDMS-based microfluidic
760 system for assessment of the protective role of dexmedetomidine against sepsis-related
761 glycocalyx degradation,” *Microfluid. Nanofluidics* **27**(5), 29 (2023).

762 ²⁸ D. Kim, and C.L. Haynes, “On-Chip Evaluation of Neutrophil Activation and Neutrophil–
763 Endothelial Cell Interaction during Neutrophil Chemotaxis,” *Anal. Chem.* **85**(22), 10787–10796
764 (2013).

765 ²⁹ F. Soroush, T. Zhang, D.J. King, Y. Tang, S. Deosarkar, B. Prabhakarpandian, L.E. Kilpatrick,
766 and M.F. Kiani, “A novel microfluidic assay reveals a key role for protein kinase C δ in
767 regulating human neutrophil–endothelium interaction,” *J. Leukoc. Biol.* **100**(5), 1027–1035
768 (2016).

769 ³⁰ S. Han, J.-J. Yan, Y. Shin, J. J. Jeon, J. Won, H.E. Jeong, R. D. Kamm, Y.-J. Kim, and S.
770 Chung, “A versatile assay for monitoring *in vivo* -like transendothelial migration of neutrophils,”
771 *Lab. Chip* **12**(20), 3861–3865 (2012).

772 ³¹ X. Wu, M.A. Newbold, and C.L. Haynes, “Recapitulation of *in vivo*-like neutrophil
773 transendothelial migration using a microfluidic platform,” *Analyst* **140**(15), 5055–5064 (2015).

774 ³² N. Venugopal Menon, H. Min Tay, S. Nan Wee, K.H. Holden Li, and H. Wei Hou, “Micro-
775 engineered perfusable 3D vasculatures for cardiovascular diseases,” *Lab. Chip* **17**(17), 2960–
776 2968 (2017).

777 ³³ P.N. Ingram, L.E. Hind, J.A. Jiminez-Torres, A. Huttenlocher, and D.J. Beebe, "An Accessible
778 Organotypic Microvessel Model Using iPSC-Derived Endothelium," *Adv. Healthc. Mater.* **7**(2),
779 1700497 (2018).

780 ³⁴ R.B. Riddle, K. Jennbacken, K.M. Hansson, and M.T. Harper, "Endothelial inflammation and
781 neutrophil transmigration are modulated by extracellular matrix composition in an inflammation-
782 on-a-chip model," *Sci. Rep.* **12**(1), 6855 (2022).

783 ³⁵ B. Baddal, and P. Marrazzo, "Refining Host-Pathogen Interactions: Organ-on-Chip Side of the
784 Coin," *Pathogens* **10**(2), 203 (2021).

785 ³⁶ F. Yokoi, S. Deguchi, and K. Takayama, "Organ-on-a-chip models for elucidating the cellular
786 biology of infectious diseases," *Biochim. Biophys. Acta BBA - Mol. Cell Res.* **1870**(6), 119504
787 (2023).

788 ³⁷ T. Feaugas, and N. Sauvonnet, "Organ-on-chip to investigate host-pathogens interactions,"
789 *Cell. Microbiol.* **23**(7), e13336 (2021).

790 ³⁸ Y. Wang, P. Wang, and J. Qin, "Microfluidic Organs-on-a-Chip for Modeling Human
791 Infectious Diseases," *Acc. Chem. Res.* **54**(18), 3550–3562 (2021).

792 ³⁹ D. Huh, B.D. Matthews, A. Mammoto, M. Montoya-Zavala, H.Y. Hsin, and D.E. Ingber,
793 "Reconstituting Organ-Level Lung Functions on a Chip," *Science* **328**(5986), 1662–1668 (2010).

794 ⁴⁰ P.H. McMinn, A. Ahmed, A. Huttenlocher, D.J. Beebe, and S.C. Kerr, "The lymphatic
795 endothelium-derived follistatin: activin A axis regulates neutrophil motility in response to
796 *Pseudomonas aeruginosa*," *Integr. Biol.* **15**, zyad003 (2023).

797 ⁴¹ K. Sharma, N. Dhar, V.V. Thacker, T.M. Simonet, F. Signorino-Gelo, G.W. Knott, and J.D.
798 McKinney, "Dynamic persistence of UPEC intracellular bacterial communities in a human
799 bladder-chip model of urinary tract infection," *eLife* **10**, e66481 (2021).

800 ⁴² F. Siwczak, Z. Cseresnyes, M.I.A. Hassan, K.O. Aina, S. Carlstedt, A. Sigmund, M. Groger,
801 B.G.J. Surewaard, O. Werz, M.T. Figge, L. Tuchscher, B. Löffler, and A.S. Mosig, “Human
802 macrophage polarization determines bacterial persistence of *Staphylococcus aureus* in a liver-on-
803 chip-based infection model,” *Biomaterials* **287**, 121632 (2022).

804 ⁴³ S. Deinhardt-Emmer, K. Rennert, E. Schicke, Z. Cseresnyés, M. Windolph, S. Nietzsche, R.
805 Heller, F. Siwczak, K.F. Haupt, S. Carlstedt, M. Schacke, M.T. Figge, C. Ehrhardt, B. Löffler,
806 and A.S. Mosig, “Co-infection with *Staphylococcus aureus* after primary influenza virus
807 infection leads to damage of the endothelium in a human alveolus-on-a-chip model,”
808 *Biofabrication* **12**(2), 025012 (2020).

809 ⁴⁴ Y. Zhu, F. Yin, H. Wang, L. Wang, J. Yuan, and J. Qin, “Placental Barrier-on-a-Chip:
810 Modeling Placental Inflammatory Responses to Bacterial Infection,” *ACS Biomater. Sci. Eng.*
811 **4**(9), 3356–3363 (2018).

812 ⁴⁵ R. Rauti, S. Navok, D. Biran, K. Tadmor, Y. Leichtmann-Bardoogo, E.Z. Ron, and B.M.
813 Maoz, “Insight on Bacterial Newborn Meningitis Using a Neurovascular-Unit-on-a-Chip,”
814 *Microbiol. Spectr.* **11**(3), e01233-23 (2023).

815 ⁴⁶ R. Plebani, R. Potla, M. Soong, H. Bai, Z. Izadifar, A. Jiang, R.N. Travis, C. Belgur, A. Dinis,
816 M.J. Cartwright, R. Prantil-Baun, P. Jolly, S.E. Gilpin, M. Romano, and D.E. Ingber, “Modeling
817 pulmonary cystic fibrosis in a human lung airway-on-a-chip,” *J. Cyst. Fibros.* **21**(4), 606–615
818 (2022).

819 ⁴⁷ Y. Du, N. Li, H. Yang, C. Luo, Y. Gong, C. Tong, Y. Gao, S. Lü, and M. Long, “Mimicking
820 liver sinusoidal structures and functions using a 3D-configured microfluidic chip,” *Lab. Chip*
821 **17**(5), 782–794 (2017).

822 ⁴⁸ R.A. Shaikh, J. Zhong, M. Lyu, S. Lin, D. Keskin, G. Zhang, L. Chitkushev, and V. Brusic, in
823 *2019 IEEE Int. Conf. Bioinforma. Biomed. BIBM* (2019), pp. 2207–2213.

824 ⁴⁹ H.J. Kim, H. Li, J.J. Collins, and D.E. Ingber, “Contributions of microbiome and mechanical
825 deformation to intestinal bacterial overgrowth and inflammation in a human gut-on-a-chip,”
826 *Proc. Natl. Acad. Sci.* **113**(1), E7–E15 (2016).

827 ⁵⁰ M. Gröger, K. Rennert, B. Giszas, E. Weiß, J. Dinger, H. Funke, M. Kiehntopf, F.T. Peters, A.
828 Lupp, M. Bauer, R.A. Claus, O. Huber, and A.S. Mosig, “Monocyte-induced recovery of
829 inflammation-associated hepatocellular dysfunction in a biochip-based human liver model,” *Sci.*
830 *Rep.* **6**(1), 21868 (2016).

831 ⁵¹ Y. Xu, S. Li, C. Wang, X. Xie, and X. Mi, “μF-hBBB Chip Together with Tetrahedral DNA
832 Frameworks for Visualization of LPS-Mediated Inflammation,” *Anal. Chem.* **95**(30), 11449–
833 11455 (2023).

834 ⁵² A. Jain, R. Barrile, A. van der Meer, A. Mammoto, T. Mammoto, K. De Ceunynck, O. Aisiku,
835 M. Otieno, C. Louden, G. Hamilton, R. Flaumenhaft, and D. Ingber, “Primary Human Lung
836 Alveolus-on-a-chip Model of Intravascular Thrombosis for Assessment of Therapeutics,” *Clin.*
837 *Pharmacol. Ther.* **103**(2), 332–340 (2018).

838 ⁵³ K.H. Benam, R. Villenave, C. Lucchesi, A. Varone, C. Hubeau, H.-H. Lee, S.E. Alves, M.
839 Salmon, T.C. Ferrante, J.C. Weaver, A. Bahinski, G.A. Hamilton, and D.E. Ingber, “Small
840 airway-on-a-chip enables analysis of human lung inflammation and drug responses *in vitro*,”
841 *Nat. Methods* **13**(2), 151–157 (2016).

842 ⁵⁴ D. Lebeaux, J.-M. Ghigo, and C. Beloin, “Biofilm-Related Infections: Bridging the Gap
843 between Clinical Management and Fundamental Aspects of Recalcitrance toward Antibiotics,”
844 *Microbiol. Mol. Biol. Rev.* **78**(3), 510–543 (2014).

845 ⁵⁵ J.W. Costerton, P.S. Stewart, and E.P. Greenberg, "Bacterial Biofilms: A Common Cause of
846 Persistent Infections," *Science* **284**(5418), 1318–1322 (1999).

847 ⁵⁶ D. Shi, G. Mi, M. Wang, and T.J. Webster, "In vitro and ex vivo systems at the forefront of
848 infection modeling and drug discovery," *Biomaterials* **198**, 228–249 (2019).

849 ⁵⁷ T. Bjarnsholt, M. Alhede, M. Alhede, S.R. Eickhardt-Sørensen, C. Moser, M. Kühl, P.Ø.
850 Jensen, and N. Høiby, "The in vivo biofilm," *Trends Microbiol.* **21**(9), 466–474 (2013).

851 ⁵⁸ K.N. Kragh, T. Tolker-Nielsen, and M. Lichtenberg, "The non-attached biofilm aggregate,"
852 *Commun. Biol.* **6**(1), 1–13 (2023).

853 ⁵⁹ A.A. Anas, W.J. Wiersinga, A.F. de Vos, and T. van der Poll, "Recent insights into the
854 pathogenesis of bacterial sepsis," *Neth. J. Med.* **68**(4), 147–152 (2010).

855 ⁶⁰ C.M. Leung, P. de Haan, K. Ronaldson-Bouchard, G.-A. Kim, J. Ko, H.S. Rho, Z. Chen, P.
856 Habibovic, N.L. Jeon, S. Takayama, M.L. Shuler, G. Vunjak-Novakovic, O. Frey, E. Verpoorte,
857 and Y.-C. Toh, "A guide to the organ-on-a-chip," *Nat. Rev. Methods Primer* **2**(1), 1–29 (2022).

858 ⁶¹ E. Vénéreau, C. Ceriotti, and M.E. Bianchi, "DAMPs from Cell Death to New Life," *Front.*
859 *Immunol.* **6**, (2015).

860 ⁶² V. Paloschi, M. Sabater-Lleal, H. Middelkamp, A. Vivas, S. Johansson, A. van der Meer, M.
861 Tenje, and L. Maegdefessel, "Organ-on-a-chip technology: a novel approach to investigate
862 cardiovascular diseases," *Cardiovasc. Res.* **117**(14), 2742–2754 (2021).

863 ⁶³ T.H. Nguyen, M.D. Park, and M. Otto, "Host Response to *Staphylococcus epidermidis*
864 Colonization and Infections," *Front. Cell. Infect. Microbiol.* **7**, 90 (2017).

865 ⁶⁴ V. Paloschi, J. Pauli, G. Winski, Z. Wu, Z. Li, L. Botti, S. Meucci, P. Conti, F. Rogowitz, N.
866 Glukha, N. Hummel, A. Busch, E. Chernogubova, H. Jin, N. Sachs, H.-H. Eckstein, A. Dueck,
867 R.A. Boon, A.R. Bausch, and L. Maegdefessel, "Utilization of an Artery-on-a-Chip to Unravel

868 Novel Regulators and Therapeutic Targets in Vascular Diseases," *Adv. Healthc. Mater.*,
869 e2302907 (2023).

870 ⁶⁵ Y. Qiu, B. Ahn, Y. Sakurai, C.E. Hansen, R. Tran, P.N. Mimche, R.G. Mannino, J.C.
871 Ciciliano, T.J. Lamb, C.H. Joiner, S.F. Ofori-Acquah, and W.A. Lam, "Microvasculature-on-a-
872 chip for the long-term study of endothelial barrier dysfunction and microvascular obstruction in
873 disease," *Nat. Biomed. Eng.* **2**(6), 453–463 (2018).

874 ⁶⁶ N.K.R. Pandian, B.K. Walther, R. Suresh, J.P. Cooke, and A. Jain, "Microengineered Human
875 Vein-Chip Recreates Venous Valve Architecture and Its Contribution to Thrombosis," *Small*
876 **16**(49), 2003401 (2020).

877 ⁶⁷ A.R. Henderson, I.S. Ilan, and E. Lee, "A bioengineered lymphatic vessel model for studying
878 lymphatic endothelial cell-cell junction and barrier function," *Microcirculation* **28**(8), e12730
879 (2021).

880 ⁶⁸ S. Chatterjee, "Endothelial Mechanotransduction, Redox Signaling and the Regulation of
881 Vascular Inflammatory Pathways," *Front. Physiol.* **9**, 524 (2018).

882 ⁶⁹ A.G. Koutsiaris, S.V. Tachmitzi, N. Batis, M.G. Kotoula, C.H. Karabatsas, E. Tsironi, and
883 D.Z. Chatzoulis, "Volume flow and wall shear stress quantification in the human conjunctival
884 capillaries and post-capillary venules *in vivo*," *Biorheology* **44**(5–6), 375–386 (2007).

885 ⁷⁰ M.L. Jackson, A.R. Bond, and S.J. George, "Mechanobiology of the endothelium in vascular
886 health and disease: *in vitro* shear stress models," *Cardiovasc. Drugs Ther.* **37**(5), 997–1010
887 (2023).

888 ⁷¹ E. Roux, P. Bougaran, P. Dufourcq, and T. Couffinhal, "Fluid Shear Stress Sensing by the
889 Endothelial Layer," *Front. Physiol.* **11**, 861 (2020).

890 ⁷² G.J. Mahler, C.M. Frendl, Q. Cao, and J.T. Butcher, “Effects of shear stress pattern and
891 magnitude on mesenchymal transformation and invasion of aortic valve endothelial cells,”
892 *Biotechnol. Bioeng.* **111**(11), 2326–2337 (2014).

893 ⁷³ D.E. Ingber, “Human organs-on-chips for disease modelling, drug development and
894 personalized medicine,” *Nat. Rev. Genet.* **23**(8), 467–491 (2022).

895 ⁷⁴ S. Biglari, T.Y.L. Le, R.P. Tan, S.G. Wise, A. Zambon, G. Codolo, M. De Bernard, M.
896 Warkiani, A. Schindeler, S. Naficy, P. Valtchev, A. Khademhosseini, and F. Dehghani,
897 “Simulating Inflammation in a Wound Microenvironment Using a Dermal Wound-on-a-Chip
898 Model,” *Adv. Healthc. Mater.* **8**(1), 1801307 (2019).

899 ⁷⁵ A.D. van der Meer, K. Vermeul, A.A. Poot, J. Feijen, and I. Vermes, “A microfluidic wound-
900 healing assay for quantifying endothelial cell migration,” *Am. J. Physiol. Heart Circ. Physiol.*
901 **298**(2), H719-725 (2010).

902 ⁷⁶ D. Sticker, S. Lechner, C. Jungreuthmayer, J. Zanghellini, and P. Ertl, “Microfluidic Migration
903 and Wound Healing Assay Based on Mechanically Induced Injuries of Defined and Highly
904 Reproducible Areas,” *Anal. Chem.* **89**(4), 2326–2333 (2017).

905 ⁷⁷ D. Leaper, O. Assadian, and C.E. Edmiston, “Approach to chronic wound infections,” *Br. J.*
906 *Dermatol.* **173**(2), 351–358 (2015).

907 ⁷⁸ D. Church, S. Elsayed, O. Reid, B. Winston, and R. Lindsay, “Burn Wound Infections,” *Clin.*
908 *Microbiol. Rev.* **19**(2), 403–434 (2006).

909 ⁷⁹ F. Shahabipour, S. Satta, M. Mahmoodi, A. Sun, N.R. De Barros, S. Li, T. Hsiai, and N.
910 Ashammakhi, “Engineering organ-on-a-chip systems to model viral infections,” *Biofabrication*
911 **15**(2), 022001 (2023).

912 ⁸⁰ H. Tang, Y. Abouleila, L. Si, A.M. Ortega-Prieto, C.L. Mummery, D.E. Ingber, and A.
913 Mashaghi, "Human Organs-on-Chips for Virology," *Trends Microbiol.* **28**(11), 934–946 (2020).

914 ⁸¹ J. Li, H. Bai, Z. Wang, B. Xu, K.N. Peters Olson, C. Liu, Y. Su, J. Hao, J. Shen, X. Xi, J.
915 Zhen, R. Yu, Y. Sun, X. Xie, W. Tian, F. Yu, X. Liu, L. Zhang, D. Zhou, and L. Si,
916 "Advancements in organs-on-chips technology for viral disease and anti-viral research," *Organs-
917 --Chip* **5**, 100030 (2023).

918 ⁸² M. Zhang, P. Wang, R. Luo, Y. Wang, Z. Li, Y. Guo, Y. Yao, M. Li, T. Tao, W. Chen, J. Han,
919 H. Liu, K. Cui, X. Zhang, Y. Zheng, and J. Qin, "Biomimetic Human Disease Model of SARS-
920 CoV-2-Induced Lung Injury and Immune Responses on Organ Chip System," *Adv. Sci.* **8**(3),
921 2002928 (2021).

922 ⁸³ J.C. Nawroth, C. Lucchesi, D. Cheng, A. Shukla, J. Ngyuen, T. Shroff, A. Varone, K. Karalis,
923 H.-H. Lee, S. Alves, G.A. Hamilton, M. Salmon, and R. Villenave, "A Microengineered Airway
924 Lung Chip Models Key Features of Viral-induced Exacerbation of Asthma," *Am. J. Respir. Cell
925 Mol. Biol.* **63**(5), 591–600 (2020).

926 ⁸⁴ S. Sun, L. Jin, Y. Zheng, and J. Zhu, "Modeling human HSV infection via a vascularized
927 immune-competent skin-on-chip platform," *Nat. Commun.* **13**(1), 5481 (2022).

928 ⁸⁵ Y.B. (Abraham) Kang, S. Rawat, N. Duchemin, M. Bouchard, and M. Noh, "Human Liver
929 Sinusoid on a Chip for Hepatitis B Virus Replication Study," *Micromachines* **8**(1), 27 (2017).

930 ⁸⁶ M. Kraft, "The role of bacterial infections in asthma," *Clin. Chest Med.* **21**(2), 301–313
931 (2000).

932 ⁸⁷ J.H. Sung, M.B. Esch, J.-M. Prot, C.J. Long, A. Smith, J.J. Hickman, and M.L. Shuler,
933 "Microfabricated mammalian organ systems and their integration into models of whole animals
934 and humans," *Lab. Chip* **13**(7), 1201–1212 (2013).

935 ⁸⁸ M.B. Esch, and G.J. Mahler, in *Microfluid. Cell Cult. Syst. Second Ed.*, edited by J.T.
936 Borenstein, V. Tandon, S.L. Tao, and J.L. Charest (Elsevier, 2019), pp. 323–350.

937 ⁸⁹ K. Ronaldson-Bouchard, D. Teles, K. Yeager, D.N. Tavakol, Y. Zhao, A. Chramiec, S.
938 Tagore, M. Summers, S. Stylianos, M. Tamargo, B.M. Lee, S.P. Halligan, E.H. Abaci, Z. Guo, J.
939 Jacków, A. Pappalardo, J. Shih, R.K. Soni, S. Sonar, C. German, A.M. Christiano, A. Califano,
940 K.K. Hirschi, C.S. Chen, A. Przekwas, and G. Vunjak-Novakovic, “A multi-organ chip with
941 matured tissue niches linked by vascular flow,” *Nat. Biomed. Eng.* **6**(4), 351–371 (2022).

942 ⁹⁰ M. Medina, H. Legido-Quigley, and L.Y. Hsu, in *Glob. Health Secur. Recognizing
943 Vulnerabilities Creat. Oppor.*, edited by A.J. Masys, R. Izurieta, and M. Reina Ortiz (Springer
944 International Publishing, Cham, 2020), pp. 209–229.

945 ⁹¹ R. Uchimido, E.P. Schmidt, and N.I. Shapiro, “The glycocalyx: a novel diagnostic and
946 therapeutic target in sepsis,” *Crit. Care* **23**, 16 (2019).

947